

State of the Art in the Control of Inclusions during Steel Ingot Casting

Authors: Dr. Lifeng Zhang, and Prof. Brian G. Thomas

Dept. of Mech. Engr., University of Illinois at Urbana-Champaign

1206 W. Green St., Urbana, IL 61801

Tel: 1-217-244-4656

Fax: 1-217-244-6534

Email: zhang25@uiuc.edu bgthomas@uiuc.edu

Corresponding author:

Dr. Lifeng Zhang

345MEB, MC244,

1206 West Green St., Urbana, IL 61801

Tel: 1-217-244-4656, Fax: 1-217-244-6534

Email: zhang25@uiuc.edu

Abstract:

This paper extensively reviews published research on inclusions in ingot steel and defects on ingot products, methods to measure and detect inclusions in steel, the causes of exogenous inclusions, and the transport and entrapment of inclusions during fluid flow, segregation and solidification of steel cast in ingot molds. Exogenous inclusions in ingots originate mainly from reoxidation of the molten steel, slag entrapment and lining erosion, which are detailed in this paper. The measures to prevent the formation of exogenous inclusions and improve their removal are provided, which are very useful for the clean steel production of ingot industries.

Key words: Steel Ingot Casting, Inclusions, Exogenous Inclusions, Steel Reoxidation, Slag Entrapment, Lining Erosion, Fluid Flow

I. INTRODUCTION

Although the percentage of steel produced in the world via ingot casting has decreased to 11.2% (**figure 1** ^[8]) in 2003, some low-alloy steel grades and steel for special applications can only be produced by this process. These include high carbon chromium bearing steel, ^[9] thick plate, seamless tube, forgings, bars and wire rods.^[7] Thus, the production of crude steel ingots in 2003 was about 2.5 million metric tonnes in USA, 17.8 million metric tonnes in China, and 108.7 million metric tonnes in the world, which is still important.

Top pouring is easy to use, but generates many defects both on the surface and internally, which is not suitable for high quality steels. Bottom pouring is better, especially for intensive deoxidation, high superheat, low-speed casting and casting in a nonoxidizing atmosphere. The typical process from steelmaking to steel refining to bottom-poured ingot casting is given in **figure 2** ^[10, 11]. During teeming, molten steel flows through the well and controlling side gate at the bottom of ladle, enters the trumpet (also called the central runner,) and passes through the spider, into the runners. The system is often flooded with inert gas (such as argon) to lessen oxidation. Molten steel then enters the ingot mold through an upward-facing ingate near the end of the runner. There, the rising steel level burns through suspended bags to release mold powder, which spreads, and melts to form a slag layer that floats on top of the molten steel to protect it from atmospheric oxidation and to absorb inclusions. After teeming, the ingot stands to solidify for the optimal time for easy removal (stripping) from the mold.

The ever-increasing demands for high quality have made the steelmaker increasingly aware of the necessity for products to meet stringent “cleanliness” requirements. Non-metallic inclusions are a significant problem in cast steels that can lead to problems in castings that require expensive casting repairs or rejection. The mechanical properties of steel are controlled to a large degree by the volume fraction, size, distribution, composition and morphology of inclusions and precipitates, which act as stress raisers. For example, ductility is appreciably decreased with increasing amounts of either oxides or sulphides. ^[12] Fracture toughness decreases when inclusions are present, especially in higher-strength lower-ductility alloys. Similar pronounced property degradation caused by inclusions is observed in tests that reflect slow, rapid, or cyclic strain rates, such as creep, impact, and fatigue testing. ^[12] **Figure 3** shows that inclusions cause voids, which will induce cracks if larger than a critical value. ^[13] Large exogenous inclusions also cause inferior surface appearance, poor polishability, reduced resistance to corrosion, and in severe cases, slag lines and

laminations.^[14] Inclusions also lower resistance to Hydrogen Induced Cracks.^[15] The source of most fatigue problems in steel are hard and brittle oxide inclusions. Larger inclusions have more negative effect on the fatigue life than smaller ones.^[9] In general, rolling contact fatigue life decreases as the total oxygen content increases^[9]. **Figure 4** shows the fatigue limit for different inclusion sizes in different strength steels.^[16]

To avoid these problems, the size and frequency of detrimental inclusions must be carefully controlled. It is especially important to ensure that there are no inclusions in the casting above a critical size. **Table I** shows some typical restrictions on inclusions in different steels.^[17] The life of bearing steels greatly depends on controlling the amount of nonmetallic inclusions, hard aluminum oxides and especially large oxides over 30 μ m.^[18-20] **Figure 5** shows the relationship between bearing life and the oxygen content of steel.^[20] Lowering the amount of large inclusions by lowering the oxygen content to 3-6ppm has extended bearing life by almost 30 times in comparison with steels with 20 ppm oxygen.

Although the solidification morphology of inclusions is of most importance in steel castings, the morphology of inclusions in wrought products is largely controlled by their mechanical behavior during steel processing, i.e., whether they are “hard” or “soft” relative to the steel matrix.^[21] Normally pure alumina inclusions are non-deformable, thus should be avoided. Calcium treatment is well known to generate deformable inclusions and can lower the number of stringers of indigenous inclusions in steel^[15, 21].

The rest of this report is an extensive review on inclusions in ingot steel, their morphology, formation mechanisms and possible remedies. Emphasis is on exogenous inclusions. Although this work is fundamental in nature, it has great practical significance.

II. INCLUSIONS IN STEEL INGOTS AND RELATED PRODUCT DEFECTS

Non-metallic inclusions in steel are classified as indigenous inclusions or exogenous inclusions according to their sources.

A. *Indigenous Inclusions in Steel*

Indigenous inclusions are deoxidation products or inclusions that precipitate during cooling and solidification. Deoxidation products cause the majority of indigenous inclusions in steel, such as alumina inclusions in low carbon Al-killed steel, and silica inclusions in Si-killed steel.^[15, 22-37] They are generated by the reaction between the dissolved oxygen and the added deoxidant, such as

aluminum and silicon. Alumina inclusions are dendritic when formed in a high oxygen environment [38-40], as pictured in **figure 6a** [39]. Cluster-type alumina inclusions from deoxidation or reoxidation, as shown in **figure 6b** [41] and **figure 7** [41], are typical of aluminum-killed steels. There also exists coral-like alumina inclusions (**figure 6c** [39]), which result from “Ostwald-ripening” [42-48] of originally dendritic or clustered alumina inclusions. Alumina inclusions readily form three-dimensional clusters via collision and aggregation due to their high interfacial energy. Individual inclusions in the cluster range from 1 -5 microns in diameter [47, 48]. Before they collide and aggregate, small alumina particles, may be in the shape of sphere, flower plate [49] or polyhedral alumina [40, 49, 50], as shown in **figure 8** [49]. Silica inclusions are generally spherical [50-52], owing to their liquid or glassy state in the molten steel. Silica inclusions can also agglomerate into clusters, as shown in **figure 9** [52].

Precipitated inclusions form during cooling and solidification of the molten steel. [9, 28, 53-59] During cooling, the concentration of dissolved oxygen/nitrogen/sulfur in the liquid becomes larger, while the solubility of these elements decreases. Thus inclusions such as alumina [59], silica, AlN [54], TiN, and sulphide precipitate. Sulphides form interdendritically during solidification, and often nucleate on oxides already present in the liquid steel. [60] These inclusions are normally small (<10µm) [53], but may form large clusters. [61] An example of sulfide inclusions (MnS) in an ingot is shown in **figure 10** [61]. **Figure 11** shows SEM and TEM micrographs of AlN inclusions in a high Al ingot ((a)(a') plate-like, (b) (b') feathery, (c)(c') branched rod-like) which formed both during and after solidification of the matrix. [54]

Figure 12 clearly shows the drop in the total oxygen from tapping to solidification of the ingot after a constant addition of various deoxidants. The differences cannot be explained solely by the different equilibrium constants for dissolved oxygen and these deoxidants, as different inclusions also have different removal rates, due to mechanisms such as flotation. [62] This figure shows that Al has the best deoxidation ability, followed by Ti, Zr, and Si is lowest. This figure also indicates that inclusions can be removed by transport to the slag layer on the top surface during teeming and subsequent standing of the ingot.

The inclusion size distribution measured in different steel ingots is shown in **figure 13**. Franklin [63] measured inclusions amounts as follows: 3-10µm dia. 3.0×10^{11} ; 10-20µm dia. 2.5×10^{10} ; 20-30µm dia. 2.4×10^9 ; 30-40µm dia. 4.5×10^8 ; 40-60µm dia. 1.0×10^8 ; 60-80µm dia. 1.0×10^7 . Miki et al measured the size distribution of large inclusions in a steel ingot by the Slime test. [52] Zhang et

al estimated the three-dimensional inclusion size distribution by converting the two-dimensional microscope observations at many different locations into 3D. ^[61] The difference between these measurements is partially due to the different bin size used. The latter measurements found fewer small inclusions, but similar numbers of large inclusions, including a significant number of very detrimental inclusions larger than 600 μm .

B. *Exogenous Inclusions in Steel*

Exogenous inclusions arise from unintended chemical and mechanical interaction of liquid steel with its surroundings. They generally have the most deleterious effect on machinability, surface quality and mechanical properties because of their large size and location near the surface. In machining, they produce chatter, causing pits and gouges on the surface of machined sections, frequent breakage, and excessive tool wear. Exogenous inclusions come mainly from reoxidation, entrained slag as shown in **figure 14**, lining erosion as shown in **figure 15**, and chemical reactions. Because they are usually entrapped accidentally during teeming and solidification, exogenous inclusions are sporadic. They easily float out, so only concentrate in regions of the steel that solidify rapidly or where their escape by fluid transport and flotation is hampered. Consequently, they are often found near the ingot surface. Possible reasons for the entrapment of these large inclusions include:

- Late formation during steelmaking or transfer, leaving insufficient time for them to rise before entering the mold;
- Inadequate or high-rate teeming systems that encourage air entrainment or erosion of the trumpet, runner, and ingate refractories.
- Insufficient superheat ^[64];
- Inferior mold design such as reverse taper, depressions in the wall of ingot, or sharp corner between wall and bottom;
- The fluid flow during ingot mold filling induces mold slag entrapment, or re-entrainment of floated inclusions before they fully enter the slag;
- Natural convection carries inclusions along the solidifying shell to the bottom of the ingot;
- The raining down of heavy equiaxed crystals may capture and carry the floating exogenous inclusions down to the bottom, or at least retard their floating.

Exogenous inclusions have the following common characteristics:

- Compound / multiphase composition (as shown in Fig.14d): Their size and composition depend on the type and order of deoxidant additions. In silicon-killed steels, for example, $\text{MnO-SiO}_2\text{-Al}_2\text{O}_3$ silicate deoxidation products interact with slag particles and pick up lime and magnesium. Calcium and magnesium aluminates can form in Al-killed steels, with compositions evolving in sequence $\text{CaO}\cdot 6(\text{Al}_2\text{O}_3)$, $\text{CaO}\cdot 2(\text{Al}_2\text{O}_3)$, $\text{CaO}\cdot \text{Al}_2\text{O}_3$, as the aluminum content decreases. In electric furnace steelmaking, an alternative source of calcium and magnesium is provided by the reduction of refractories in heats made with strongly reducing slags. ^[21] The following phenomena account for the complicated composition of exogenous inclusions.
- Exogenous inclusions act as heterogeneous nucleus sites for precipitation of new inclusions during their motion in molten steel (**figure16a** ^[65]);
- As exogenous inclusions move through the molten steel, due to their large size, they may entrap deoxidation inclusions such as Al_2O_3 on their surface (Fig. 14c and **figure 16b** ^[66]);
- Reactions between molten steel and SiO_2 , FeO , and MnO in the slag and lining refractory, can further augment inclusions transported near to the slag-metal interface;
- Slag or reoxidation inclusions may react with the lining refractories or dislodge further material into the steel.
- Large size (usually $>50\mu\text{m}$) : The maximum observed size of inclusions in steel is given in **figure 17** ^[51], which also indicates that inclusions from refractory erosion are generally larger than those from slag entrainment.
- Irregular shape: differing from the spherical shape of entrained slag and small, single-phase deoxidation product particles. .
- Small number and low mass fraction, compared with small inclusions.
- Sporadic distribution in the steel, contrasting with the even dispersal of small inclusions.
- More deleterious to steel properties, because of their large size.

The frequency of exogenous inclusions in slabs and plates forged from ingots is exemplified in **Table III** ^[14] and Fig.13. Table III also shows that hot rolling and forging processes elongate the ingot inclusions to form stringers, which are longer in plates than in slabs, due to the greater thickness reduction .

Exogenous inclusions always depend on the steelmaking and teeming practices, so their size, shape, and chemical composition often allow their source to be identified. Once the inclusion source is found, an effective process change usually can be made to eliminate that particular problem in the future. Unfortunately, exogenous inclusions often originate from a combination of several sources, so methods for their prevention are seldom simple. In addition to the features already discussed, consideration should be given to runner system and ingot shape design, hot-topping systems, teeming temperatures and teeming rates. Only through attention to all inclusion sources and removal mechanisms can the incidence of large non-metallic inclusions in steels be reduced.

C. *Defects in Ingot Steel Products*

Three books / sections have extensively discussed steel-product defects. British Iron and Steel Research Association compiled a compendium of surface defects in ingots and their products in 1958^[67], and defined the causes of continuous casting defects in 1967^[68]. Ginzburg and Ballas reviewed the defects in cast slabs and hot rolled products, many of which are related to inclusions.^[69] Some of the defects in steel products, such as scaling, arise during rolling.^[69] This section reviews only those defects related to inclusions in ingot casting, which include slag spots, line defects, slivers, blisters, pencil pipe, laps, and laminations.

Two types of exogenous slag spots have been observed. The first^[70-73] contain calcium, magnesium, aluminum and oxygen and the second^[70-72] additionally contain ,magnesium. An example slag spot on a cold rolled sheet is shown in **figure 18**^[73].

Line defects or “slivers” appear on the surface of finished strip product, with widths of several tens of micrometers to millimeter and as long as 0.1-1 meter^[74]. This surface defect is believed to result from rolling nonmetallic inclusions caught near the surface of the ingot or slab (<15mm from the surface). This defect is called blisters or pencil pipe if coupled with elongated bubbles. Three major types of line defects on cold rolled sheets from steelmaking and casting sources include: (a) iron oxide^[70-72], (b) alumina^[70-72] and (c) exogenous oxide inclusions.^[67, 70-77], such as mold slag^[70-72, 77]. Examples are given in **figure 19**^[75]. If the inclusions in these line defects include hard particles such as galaxite, chrome-galaxite or spinels, then polishing the sheet may dislodge some of them and cause scratch marks (Fig. 19b).^[75] Metallographic examination of pickled plate ends may reveal subsurface ‘tunnel’ defects,, also called laps, such as shown in **figure 20**^[75]. Optical microscopy and microanalysis found traces of silicate inclusions remaining in some tunnels, which indicates they likely form when silicate-galaxite inclusions are exposed at the surface of the plate

during rolling and are progressively dissolved away during subsequent pickling to leave the tunnels.
[75]

If a sliver defect in a strip rolled from ingot steel is very severe, such as shown in **figure 21a**, its outer steel layer may tear away or “delaminate” from the surface^[67], generating a defect called a “lamination”. Such a “band” of defects was reported in rolled sheets of 08Yu steel, that was 25-30mm in width and tens of meters in length.^[78] The source of this severe line defect was suggested to be oxides in surface cracks and clusters of inclusions in the surface layer of the ingot, which acted as substrates to form the bands during initial rolling. **Figure 21** shows examples of line defects, including laminations. Most (60-70%) of the laminations in steel continuous-cast products are from mold slag^[76], 20-30% from alumina clusters, and 5-10% are pure FeO. Laminations are often combinations of bubble(s) and inclusions.^[67, 74]

If an elongated gas pocket entrapped below the surface of a rolled plate expands during annealing to form a smooth, slightly-raised surface (ridge), the defect is called a “pencil blister”.^[74], which originates from “blow hole”, or “pin hole” in the as-cast ingot. This surface defect has a tubular shape, typically ~1mm wide and 150-300mm long^[74, 77], such as shown in **figure 21d**. It originates when a bubble is entrapped during casting and elongates into a gas pocket during annealing. Inclusions usually attach to the surface of the bubble during its motion through the molten steel, which worsen this defect. An example of a bubble with attached inclusions is shown in **figure 22**.^[61, 79] Zhang and Taniguchi published an extensive literature review^[80, 81] and water model study^[82] on the interaction between inclusions and bubbles in molten steel.

II. METHODS TO DETECT INCLUSIONS

The amount, size distribution, shape and composition of inclusions should be measured at all stages in steel production. Measurement techniques range from direct methods, which are accurate but costly, to indirect methods, which are fast and inexpensive, but are only reliable as relative indicators. Dawson et al reviewed 9 methods in 1988 by dividing them into two categories of “off-line” methods and “online” methods.^[83-90] Zhang and Thomas reviewed around 30 methods to detect inclusions in steel.^[17]

A. *Direct Methods*

There are several direct methods to evaluate steel cleanliness. Several traditional methods directly evaluate inclusions in two-dimensional sections through solidified product samples,

including Metallograph Microscope Observation ^[16, 84, 91, 92], Image Analysis ^[14, 16, 93], Sulfur Print^[94, 95], Scanning Electron Microscopy ^[39, 96], Optical Emission Spectrometry with Pulse Discrimination Analysis ^[95, 97-100], Laser Microprobe Mass Spectrometry ^[101], X-ray Photoelectron Spectroscopy ^[96], Auger Electron Spectroscopy ^[96], and Cathodoluminescence Microscope^[73]. Several methods directly measure inclusions in the three-dimensional steel matrix. Several of these scan through the sample with ultrasound or x-rays: Conventional Ultrasonic Scanning ^[18, 19, 102, 103], Mannesmann Inclusion Detection by Analysis Surfboards ^[104] (also called Liquid Sampling Hot Rolling method.^[11, 95, 105]), Scanning Acoustic Microscope ^[106], X-ray Detection ^[87, 107-110], Chemical Dissolution ^[39, 65, 86, 111], Slime (Electrolysis) ^[86, 94, 100, 112], Electron Beam melting ^[113, 114], Cold Crucible melting^[95], Fractional Thermal Decomposition ^[100], and Magnetic Particle Inspection. ^[85, 115, 116] Several methods determine the 3-dimensional inclusion size distributions after the inclusions are extracted from the steel: Coulter Counter Analysis^[117], Photo Scattering Method^[92, 118], Laser-Diffraction Particle Size Analyzer^[95]. Several methods directly detect the inclusion amount and size distribution in the molten melt: Ultrasonic Techniques for Liquid System ^[90, 119-121], Liquid Metal Cleanliness Analyzer ^[121, 122], Confocal Scanning Laser Microscope ^[123-125], and Electromagnetic Visualization ^[126].

B. *Indirect Methods*

Owing to the cost, time requirements, and sampling difficulties of direct inclusion measurements, steel cleanliness is generally measured in the steel industry using total oxygen, nitrogen pick-up, and other indirect methods.

1. *Total oxygen measurement* ^[127-129]

The total oxygen (T.O.) in the steel is the sum of the free oxygen (dissolved oxygen) and the oxygen combined as non-metallic inclusions. Free oxygen, or “active” oxygen can be measured relatively easily using oxygen sensors. It is controlled mainly by equilibrium thermodynamics with deoxidizing elements such as aluminum. Because the free oxygen does not vary much (3-5ppm at 1600°C for Al-killed steel ^[130, 131]), the total oxygen is a reasonable indirect measure of the total amount of oxide inclusions in the steel. Due to the small amount of large inclusions in the steel and the small sample size for T.O. measurement (normally 20g), it is rare to find a large inclusion in the sample. Even if a sample has a large inclusion, it is likely discounted due to its anomalously high reading. Thus, T.O. content really represents the level of small oxide inclusions only.

2. *Nitrogen pickup*

The difference in nitrogen content between steelmaking vessels is an indicator of the air entrained during transfer operations. For example, Weirton restricted nitrogen pickup from ladle to tundish to less than 10 ppm for critical clean steel applications.^[132, 133] After deoxidation, the low dissolved oxygen content of the steel enables rapid absorption of air. Nitrogen pickup thus serves as a crude indirect measure of total oxygen, steel cleanliness, and quality problems from reoxidation inclusions.

3. *Concentration measurement for some elements*

For Low-Carbon-Aluminum-Killed (LCAK) steels, a drop in the dissolved aluminum content also indicates that reoxidation has occurred. However, this indicator is a less accurate measure than nitrogen pickup because Al can also be reoxidized by slag. Silicon pickup and manganese pickup can be used to evaluate reoxidation as well.

4. *Slag composition measurement*

Firstly, analysis of the slag composition evolution by measurements before and after operations can be interpreted to estimate inclusion absorption to the slag. Secondly, the origin of a complex oxide inclusion can be traced to slag entrainment by matching the mineral and element fractions in the slag with the inclusion composition.^[94] These methods are not easy, however, due to sampling difficulties and because changes in the thermodynamic equilibrium must be taken into account.

5. *Lining refractory*^[76, 134-139]

Analysis of the lining refractory composition before and after operations can be used to estimate inclusion absorption to the lining and the lining erosion. Also, the origin of a complex oxide inclusion can be traced to lining refractory erosion by matching the mineral and element fractions in the slag with the inclusion composition.^[94]

6. *Tracer Studies for Slag Entrainment and Lining Erosion*^[70, 76, 77, 108, 140-146]

Tracer oxides can be added into slags and linings in the ladle, tundish, trumpet, runners, mold, or hot-top compounds. Typical inclusions in the steel are then analyzed by SEM and other methods. The presence of tracer oxides in these inclusions thus reveals their source. Tracer metals such as La can also be added into molten steel before and during steel deoxidation to study the evolution and distribution of deoxidation-based inclusions in ingot^[108] and in slab^[144]. Several such tracer studies are summarized in **Table IV**.

The ultimate measure of cleanliness is to use destructive mechanical tests to measure strength, formability, deep-drawing, and / or bending properties of the final sheet product, or fatigue life of test specimens or product samples. Other sheet tests include the Hydrogen Induced Crack test and magnetoscopy.^[104] Another is the inclusion inspection in ultra-sonic fatigue test.^[147] These tests reveal the true effects of inclusions, including the potential benefit of very small inclusions ($< 1\mu\text{m}$), which should not count against cleanliness.

The previous discussion shows that there is no single ideal method to evaluate steel cleanliness. Some methods are better for quality monitoring while others are better for problem investigation. Thus, it is necessary to combine several methods together to give a more accurate evaluation of steel cleanliness in a given operation. For example, Nippon Steel used total oxygen measurement and EB melting for small inclusions, and Slime method and EB-EV for large inclusions.^[100] Baosteel employed total oxygen measurement, MMO, XPS, and SEM for small inclusions, Slime and SEM for large inclusions, nitrogen pickup for reoxidation, and slag composition analysis to investigate inclusion absorption and slag entrainment.^[94] Finally, Ultrasonic Scanning, Microscope Observation, Sulfur Printing, Slime Electrolysis, X-ray, SEM, Slag Composition Analysis, and Refractory Observation are suitable methods to detect exogenous inclusions.

III. FORMATION MECHANISMS OF EXOGENOUS INCLUSIONS

Exogenous inclusions in steel ingot casting have many sources, which have been the subject of several plant studies. Thomas et al ^[148] investigated the sources of exogenous nonmetallic inclusions in 25 heats of steel ingots and identified that 77% of the heats were affected by reoxidation products, 46% by hot top refractories, 38% by ingot top crust, 35% by hot topping compounds, 8% by slag, and 23% by others. An evaluation of various macroinclusion sources by Leach found that lining erosion is the most serious problem, as ranked in **Table II**^[75]. Cramb extensively reviewed inclusion formation in foundry processing, and found exogenous inclusions form mainly from reoxidation, slag entrainment and lining erosion.^[149] An investigation by Blair et al found similar sources of macroinclusions in high alloy steel ingot casting: 43% by reoxidation, 35% by molding materials, 14% by refractory lining, and 3% by slag.^[4] The rejection rate of steel rounds for ball bearings was reduced greatly by improving refractories, improving mold flux, preventing slag entrapment, using bottom pouring casting, and modifying roll pass design.^[150] The following sections further explore the most important formation mechanisms.

A. *Reoxidation Mechanisms*

Reoxidation during teeming is a major source of exogenous inclusions in ingot steel. ^[21] Reoxidation products are also the most common form of large macro-inclusions in foundry castings, such as the alumina clusters shown in Fig.6. The stages in formation of alumina clusters are shown in **figure 23** ^[21], including the evolution of the clusters by Si and Mn. Alumina clusters can also form by deoxidation. ^[39]

Air is the most common source of reoxidation, which can enter ingot steel in many ways:

- Molten steel mixes with air during teeming due to the strong turbulence. The major variables affecting this reoxidation mechanism are teeming speed, stream size and shape ^[64].
- Air is sucked into the molten steel at the connection between the ladle and trumpet;
- Air penetrates into the steel from the top surface of the ingot during teeming or standing.

The exposure of molten steel to the atmosphere in this manner rapidly forms oxide films on the surface of the flowing liquid, which are folded into the liquid, forming weak planes of oxide particles in the solidified product; ^[151] Severe reoxidation may cause surface scums or natural slags. These slags have very low interfacial tensions and very low viscosities, so they are easily emulsified in regions of turbulence. This leads to internal inclusions, which may separate to interfaces between the slag/lining and steel. Thus it is not unusual to see large macro-inclusions which contain both refractory materials and reoxidation products. Deoxidizing elements, like Al, Ca, Si, etc, are preferentially oxidized by environmental oxygen and their oxide products develop into non-metallic inclusions generally one to two magnitudes larger than deoxidation inclusions ^[152] Severe reoxidation can form inclusions containing FeO and MnO.

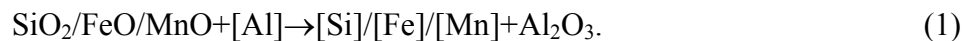
The best solution to prevent reoxidation is to limit the exposure of air to the casting process. Several different devices to protect the teeming stream protection are employed in ingot casting practice, which can be classified into four general types:

- Shrouding by an inert gas curtain injected through a steel ring manifold or porous refractory ring around the teeming nozzle; ^[153, 154]
- Intermediate shroud box seated on top of the trumpet with injection of inert gas either directly or through a porous refractory ring;
- Purging inert gas into the runner system and mold before teeming; ^[153, 155]

- Teeming in a vacuum.^[156]

Argon is a much better inert gas to prevent reoxidation than carbon dioxide^[155] or nitrogen, which are subject to other detrimental reactions.^[152, 155] Schlatter reviewed teeming stream protection systems for ingot casting, and evaluated sealing methods between teeming nozzle and trumpet, mold purging, and flooding the slide gate box with inert gas.^[152] Examples of effective sealing systems are shown in **figure 24**^[152]. Sealing was reported to lower the nitrogen content by ~30ppm and hydrogen by ~1ppm, relative to nonsealed casting, and to considerably lower large nonmetallic Al₂O₃ clusters (**figure 25**).^[7] Most significantly, sealing can improve bottom poured ingot casting quality by lowering large inclusions, especially in the interior.

Another reoxidation source is SiO₂, FeO, and MnO in the slags and lining refractories. These oxides readily react with more powerful deoxidants such as aluminum within the steel to grow inclusions near the slag or lining interface via



This leads to larger alumina inclusions with variable composition. This phenomenon further affects exogenous inclusions in the following ways:

- This reaction can erode the surface of the lining, changing its shape to alter the fluid flow pattern near the lining walls and inducing further, accelerated lining erosion;
- A large exogenous inclusion of broken lining or entrained slag can entrap small inclusions, such as deoxidation products, which may also act as a heterogeneous nucleus for further inclusion growth via precipitation. This complicates the composition of exogenous inclusions.

To prevent reoxidation from the slag or lining refractory, it is important to maintain a low FeO, MnO, and SiO₂ content. It was reported that high Al₂O₃ or zirconia bricks containing low levels of free SiO₂ are more suitable.^[7] Although high Al₂O₃ or basic bricks have good anti-erosion quality, they can combine with water in the refractory to cause blow holes in the ingot bottom unless they are first “burnt” or dried.^[7]

B. *Slag Entrainment Mechanisms*

Mold powder is added to the top surface of the molten steel in the ingot to: provide thermal insulation; protect from reoxidation; feed liquid flux into the mold shell gap for lubrication and uniform heat transfer; and assimilate any inclusions which may float (????check references)^[157-159].

Without mold powder, an oxide scum forms on the surface of the metal as it rises in the mold. This is more prominent in steels containing aluminum and titanium, where the scum formed is heavy and viscous. The scum may attach to the mold wall and become entrapped by rising metal just below the ingot surface, giving rise to surface defects and sub-surface inclusions.^[160] Refractories usually interact with the scum, which alters their mineralogical compositions by the end of casting, as shown in **figure 26**^[161]. The scums contain slightly more other oxides than the altered refractories, which are mainly alumina-silica.^[108, 161]

Any steelmaking operation involving turbulent mixing of slag and metal, especially during transfer between vessels, produces liquid slag particles suspended in the steel.^[51, 162] Many liquid particles can coalesce and be removed by transport and floatation to the top surface and absorption into the slag. However, those which remain can nucleate further inclusions and interact chemically with refractories, giving rise to complex inclusions which contain both indigenous and exogenous material. Being liquid, slag inclusions are usually spherical^[50, 53, 163], as shown in Fig.14^[50, 53].

Emulsification of liquid slags or scums on the surface of liquid steels is one of the major sources of exogenous inclusions formation.^[164] Slag inclusions, 10-300 μm in size, contain large amounts of CaO or MgO^[64], and are generally liquid at the temperature of molten steel, so are spherical in shape. Entrainment of slag occurs due to shear at the slag-metal interface caused by fluid flow, related to the sub-meniscus fluid velocity, the shear length (often related to slag depth) and the slag physical properties (density, viscosity, and surface tension). Emulsification of the slag layers which float on the top of molten steel in gas-stirred vessels has been extensively investigated.^[165-167] For the bottom pouring ingot casting process, slag entrainment into the molten steel in mold is affected mainly by the following: vortexing, method of powder addition, runner and ingate design, filling rate, turbulence at the meniscus, and slag properties.

1. *Vortex during steel pouring from a ladle*

Vortexing can entrain ladle slag into the molten steel which then flows through trumpet and runner into the mold. Sankaranarayanan and Guthrie studied vortexing during drainage in a water model of a ladle and reported that a vortex forms more easily as the liquid depth in the vessel drops, and that increasing rotational velocities at the fluid surface greatly increased the critical depth.^[168] Manabu, et. al. documented the existence of a critical gas flow rate for entrainment in both a silicon oil - water and a slag - steel system.^[169] Slag depth, slag properties, and gas bubble diameter also play a role^[169].. This vortex can be avoided in many ways, such as shutting off pouring before the

depth is too shallow, controlling the flow pattern, and / or inserting objects such as a stopper rod above the outlet to act as a vortex breaker.

2. Method of the powder addition

The best way to add the mold powder during bottom pouring is to suspend a bag containing the powder at an optimized distance such as 300mm (12 in) ^[5, 170] above the ingot bottom before teeming, as shown in Fig.2. An alternative procedure is simply to drop the bag of powder into the ingot mould before the start of pouring, whereupon the incoming steel ruptures the bag and the powder distributes itself over the surface of the steel. In this method, however, the steel is prone to engulf the powder producing defects at the bottom of the ingot, as shown in **figure 27**. Bartholomew et al (1986) ^[5] recommend use of “board flux”. This board is placed flat on the mold bottom and minimizes splash while it floats on the rising meniscus, progressively breaking down into a flux, with the same properties as a powdered mold flux. Rejections on ingots using the board flux were 0.65% while all other bottom pour ingots using powder fluxes had rejections of 1.90%. ^[5]

3. Runner and ingate design

During the initial entry of steel into the mold, the momentum of the powerful inflow jet can spout upward into the mold and entrain mold powder, if the filling rate is too high. After the initial spout has settled into a flat top surface, the incoming jet of steel may still push the floating mold powder to the sides, creating a bare surface or “eye” above the ingate. Excessive turbulence at the slag metal interface is one of the causes of reoxidation and exogenous inclusions. When interfacial level fluctuations exceed a critical level, slag entrainment will take place just inside the mold. This effect can be decreased by optimizing the runner and ingate design that delivers metal into ingot the mold cavity . ^[7, 140, 171-173] The effect of the runner outlet (mold ingate) shape on the molten steel flow pattern in the mold was examined using a water model, indicating that the ratio of the linear length of the ingate to its minimum diameter should be larger than 6, to avoid defected flow. ^[7] The direction and velocity of the inlet jet depends on the details of the ingate geometry ^[171] The flow of fluid from an upgate into a typical bottom-teemed ingot is shown in **figure 28**. ^[173] This recent computational result illustrates the great importance of ingate shape on the direction of the spout.

4. Filling rate

The filling rate is typically controlled to maintain the rate of rise of steel level in the ingot mold, between 0.2-0.3m/min (8-12 inches per minute). Large ingots, forging ingots or special designs are

usually filled slower, which is reportedly done to ensure forming a proper skin thickness to eliminate or minimize cracking. ^[5] Ogurtsov studied the importance of bottom pouring rate on ingot quality. ^[174] Fast teeming speeds increase flux entrapment, ingot cracking, defects on the ingot bottom from steel surge, choking off the steel in the refractory runner system due to the high volume of steel entering the trumpet, and recurring defects called “teeming laps” ^[67]. On the other hand, slow teeming speeds give rise to lapping or rippling surface defects, crusting of the steel meniscus, freeze-off in the refractory runner system and poor mold flux performance. The effect of the filling velocity through the ingate on the spout shape into the mold is shown in **figure 29** ^[175]. If the velocity is larger than the critical value, the metal column will enter the mold, and the steel will fall back under gravity, so slag entrainment and air absorption will take place. This critical velocity depends on steel surface tension and steel density according to ^[176] $V_{Cr}=3.5(\gamma/\rho)^{0.25}$, where typically $\gamma=1.89$ N/m, $\rho=7020\text{kg/m}^3$, $V_{Cr}=0.45\text{m/s}$. The critical filling rate can be found from this critical velocity and the ingot geometry. It is recommended that during the first several minutes, the teeming rate is kept below this critical value, and after there is a reasonable height of molten steel in mold with a stable surface level, the teeming rate can be increased gradually.

5. *Turbulence at meniscus*

Fluctuations of the meniscus level caused by surface turbulence encourage entrainment of slag droplets into the steel, leading to inclusions. Such fluctuations also enhance reoxidation by bringing the steel interface in contact with the atmosphere, or by increasing the rate of interfacial chemical reactions, including the oxidation of aluminum in the steel by iron oxide in the slag.

6. *Slag properties such as interfacial tension.*

Emulsification and slag entrainment are easier with lower interfacial tension, lower slag viscosity, and higher slag density (closer to steel). ^[177] The interfacial tension between the steel and the molten casting powder determines the shape of the steel meniscus, and the ease of flux entrainment. ^[170] Specifically, an interfacial tension of 1.4N/m for a lime-silica-alumina slag in contact with pure iron generates a meniscus height of about 8 mm (0.3in). The interfacial tension is greatly reduced by chemical reactions at the interface, or when surface-active species such as sulfur are present. A very low local interfacial tension can produce surface tension gradients, which cause spontaneous fluid flow and turbulence at the interface through the Marangoni effect. Such turbulence might emulsify the interface, and entrain slag inclusions into the steel. It should be mentioned that during molten steel sampling to investigate the steel cleanliness of an ingot, air

absorption and slag entrainment may also take place, which has been investigated by Fuchs and Jonson^[9] and Dekkers et al^[59].

C. Lining Refractory Erosion/Corrosion Mechanisms During Steel Pouring

Exogeneous inclusions generated during steel pouring include well block sand, loose dirt, broken refractory brickwork and ceramic lining particles. They are generally large and irregular-shaped^[40, 75, 108, 178, 179], as shown in Fig. 15^[40, 61, 75]. These detrimental inclusions are introduced mechanically or by chemical erosion and can completely impair the quality of an otherwise very clean steel. Erosion of refractories is a very common source of large exogenous inclusions which are typically solid and based on the materials of the trumpet, runner and mold themselves. Exogenous inclusions have been observed in ingot steel from runner erosion^[179], and as an ingot surface defect of floating slag patches from fluxed runner brick.^[67] In general, larger inclusions cause greater quality problems. The relative volumes of various inclusions can be taken as an index of their likely deleterious nature,^[51] shown in **Table V**. These numbers clearly show that erosion products are likely to cause the most problems.^[51] Almost 60% of all exogenous inclusions in killed steels are reported to arise from “attacking” or “fluxing” of refractories.^[180]

Brick quality of both the trumpet and runners has a significant effect on steel quality. The results of corrosion tests on various brick materials with high manganese steel are illustrated in **figure 30**.^[7] Erosion experiments that immersed lining samples into a melt (steel melt^[134-137] or slag melt^[76, 138, 139]) found that “glazed refractories” and “reaction layers at the surface of bricks” formed with molten steel at 1550-1600°C.^[137, 139, 180] The compositions of manganese aluminosilicate inclusions (MnO-Al₂O₃-SiO₂ system) found in forgings, ladle glaze analysis and reaction layers formed between refractory and liquid steel are compared in **figure 31**^[75]. Almost all of the inclusions in a tool steel ingot originated as oxides from the erosion of the ladle glaze, and the amount of inclusions increased with ladle age (number of heats ladle being used)^[181-183]

The interface between K1040 Al-killed steel and runner refractory is examined in **figure 32**.^[64] The metal prills are believed to occur during teeming due to the turbulence and mixing. Alumina from deoxidation products has apparently become integrated with the refractory, forming a composition gradient across the interface. Large inclusion clogs on the surface of the lining can also be released into the molten steel. **Figure 33** shows the sand build-up at the ladle side-wall.^[73]

Lining erosion generally occurs at areas of turbulent flow, especially when combined with reoxidation, high pouring temperatures, and chemical reactions. A typical defect from runner

erosion is shown in **figure 34a**.^[51] It is clear that when refractory erosion problems are likely, particular attention should be paid to the quality of the bricks.^[51] The following parameters strongly affect lining erosion:

- Some steel grades are quite corrosive (such as high-manganese steel or semi-killed grades with high soluble oxygen contents) and attack trumpet lining, runner bricks, mold insulation boards of ingot systems, or the binder and mold sands of foundry systems, leading to large entrapped particles.
- Manganese oxide preferentially attacks the silica-containing portions of the refractory. High purity (expensive) Al_2O_3 and ZrO_2 refractories can better withstand MnO slag or high-Mn steel.^[7, 134]
- Iron-oxide based inclusions are very reactive and wet the lining materials, leading to erosion of the mold in regions of high turbulence. To avoid FeO, oxygen should be minimized by fully killing the steel with a strong deoxidant such as Al or Ca, and by preventing air absorption and other reoxidation sources.
- The dissolved aluminum in steel can reduce the SiO_2 in lining refractory to form exogenous alumina inclusions via Eq. (1), so aluminosilicates such as fireclay bricks ($>60\% \text{Al}_2\text{O}_3$, $>30\% \text{SiO}_2$) should be avoided in the runners of bottom-poured ingots of high-Mn and high-Al steels.^[51] ^[140]
- Excessive velocity of molten steel along the trumpet and runner walls increases erosion / corrosion problems and the resulting macro-inclusions. Running systems should be designed to keep the velocity less than 1.0 m/s ^[140] and to minimize agitation of the metal stream.. Fast filling of the mold with low-velocity ingates minimizes erosion, such as achieved with multiple ingate systems.^[140]
- Excessive time of contact or filling and high temperature worsens erosion problems. Although it helps to float out inclusions, longer holding time in the ladle tends to increase erosion of the ladle lining by the steel. Figure 34b shows that erosion products increase in size as teeming progresses, or with prolonged teeming times. Solutions include higher-stability refractories, dense wear resistant refractory inserts for high flow areas, and preventing reoxidation.^[51]

Some erosion products also contain alumina. In laboratory experiments, mullite may arise from reaction with aluminum. Usually, alumina is produced by erosion reactions, forming corundum in the surface layers of aluminosilicate refractories, particularly at low pressure.^[51]

D. *Chemical Reaction Mechanisms*

Chemical reactions produce oxides from inclusion modification, such as when Ca treatment is improperly performed.^[12, 15, 184-186] Identifying the source is not always easy because, for example, inclusions containing CaO may also originate from entrained slag.^[184]

IV. INCLUSION AGGLOMERATION AND CLOGGING DURING STEEL POURING

The agglomeration of solid inclusions can occur on any surface, including lining refractory walls and bubble surfaces, as shown in Fig.22. This “clogging” process is greatly affected by surface tension and temperature effects. The high contact angle of alumina in liquid steel (134-146 degrees) encourages an inclusion to attach to refractory, in order to minimize its contact with steel. Temperatures above 1530°C enable alumina to sinter.^[52, 65, 187] while lowering temperature allows solid inclusions to precipitate. The effect of contact angle, particle radius, and ferrostatic pressure on the strength of an agglomeration is shown in **figure 35**^[23]. Due to collision and agglomeration, inclusions in steel tend to grow with increasing time^[52] and temperature (Fig.7^[41]).

Inclusion growth by collision, agglomeration and coagulation was investigated during ingot casting by many researchers.^[41, 188, 189] Miki et al observed SiO₂ inclusion growth by collision in a 10kg Si/Mn deoxidized steel ingot in a alumina crucible and stirred by electro-magnetic field.(Fig.9)^[188]. OOI et al investigated alumina cluster inclusions in a 20kg Al-killed steel ingot in an induction stirred crucible (Fig.7).^[41] Aritomi and Gunji found dendritic inclusion formation on a spherical primary silica in Fe-10% Ni alloy deoxidized with silicon (**Figure 36**).^[189] Several models simulate inclusion growth by collision, including recent studies by Zhang et al, which also include inclusion nucleation starting from deoxidant addition^[47, 48] The fundamentals of alumina sintering into clusters^[52, 65, 187] needs further investigation, though fractal theory has been used to describe the cluster morphology (features).^[190, 191]

Inclusion agglomeration can cause clogging problems in both nozzles and ingot runners. An example is shown in **figure 37a**^[39] and **b**^[40] of alumina inclusions clogging a submerged entry nozzle in continuous casting. Cures for this problem include improving steel cleanliness by improving ladle practices, using smooth, non-reacting refractories and controlling fluid flow to

ensure a smooth flow pattern. In 1949, Snow and Shea found Al_2O_3 covering the bore surface of nozzles used to teem Al-killed steel ingots.^[192] Duderstadt et. al. (1967)^[193] found that nozzle blockage contained high levels of Al (0.0036%) and that nozzle sectioning revealed dendritic growth of alumina from the nozzle wall onto the bore. Farrell and Hilty (1971)^[194] observed clogs of Al, Zr, Ti and rare earth metals. Many other researchers experimentally investigated nozzle clogging by alumina inclusions in steel, such as Schwerdtfeger and Schrewe (1970)^[195], Steinmetz and Lindberg (1977)^[196], Saxena et. al. (1978)^[197], Byrne and Cramb (1985)^[70-72], Dawson (1990)^[198], Fukuda et. al. (1992)^[199], Tiekink et. al. (1994)^[200], Tsujino et al (1994)^[136], Ichikawa et. al. (1994)^[201], Fuhr et al (2003)^[202]. The cause and prevention of SEN clogging was extensively reviewed by Kemeny^[203] and Thomas^[204].

V. INCLUSION TRANSPORT AND CAPTURE IN INGOT CASTING

Inclusion motion and particle entrapment depends on fluid flow, heat transfer and solidification of steel in the ingot. These phenomena in turn depend on teeming rate, runner outlet shape, ingot dimensions (height, thickness, width, taper, height-thickness ratio), wall lining refractory and mold top slag.^[7] Mathematical models of fluid flow and heat transfer are extensively used in steel search.^[205-211] **Table VI** summarizes physical^[212] and mathematical modeling studies of fluid flow, heat transfer, solidification and particle motion during ingot mold filling. In these studies of plate-shaped or small foundry ingots, the K- ϵ two-equation model is used to model turbulence, and the VOF model^[213, 214] is used to simulate the top surface rising during mold filling. Example results in Fig. 29 show the detrimental spout of excessive filling rate, compared with the flat surface of gradual filling, that presumably would generate fewer inclusion defects. Studies of three dimensional fluid flow, heat transfer, solidification, and particle motion during mold filling for a large steel ingot are rare.

Many studies of segregation during ingot solidification have been reported. The well-known internal defects of V and inverse-V segregation, central porosity, and internal inclusions, are affected by fluid flow, heat transfer, solute transport, and ingot shape. Delorme et al^[215] extensively studied the solidification of large forging ingots, segregation and macroinclusions in ingots.^[215] Tsuchida et al investigated the influence of ingot shape and composition on inverse-V segregation in 5-40t Al-killed steel ingots.^[216] Moore and Shah reviewed theories of V- and inverse V-segregation and noted the importance of interactions among fluid flow, heat transfer, and composition.^[217] Ohnaka and Matsumoto simulated macrosegregation directly in ingots.^[218]

Porosity is often found in the center of forging ingots together with “V” segregation. ^[219, 220] Many researchers have correlated porosity with temperature gradient and solidification rate. Yamada et al related porosity to the height to width ratio, of the semi-solid region formed during solidification of the ingot center. ^[219] Beckermann et al modeled both V and inverse segregation including crystal motion. ^[221, 222] Thomas et al modeled heat flow and stress in steel ingot casting to investigate panel crack formation. ^[223-225] Flemings ^[226] and Beckermann ^[221] extensively reviewed macrosegregation in steel. Maheshwari et al ^[138] and Deng ^[227] related the inclusion distribution in ingots to segregation. Zhul’ev and Zyuban investigated the effect of process parameters in the casting of large forging ingots on the formation of the optimum structure in the axial zone. ^[228] Tyurin et al studied the macrostructure of large forging ingots (~450mm in diameter and >2000mm in length). ^[229] **Figure 38** shows the simulated 2-D fluid flow pattern and macrosegregation in a Fe-0.19%C ingot ^[218]. **Figure 39** compares the solidification of conventional ingot melting and ESR process. ^[230] These figures show how the interior of conventional ingots is prone to trapping liquid in the central region, which is responsible for porosity, internal inclusions and other problems.

Inclusion distribution in an ingot is affected by fluid flow, heat transfer and solidification of the steel. A popular index for inclusion entrapment is the critical advancing velocity of the solidification front, which is affected by: inclusion shape, density, surface energy, thermal conductivity, cooling rate (solidification rate^[108]), drag and interfacial forces ^[125, 231-234] and protruding conditions of the solidification front^[108]. The probability of entrapment decreases with increasing solidification time (slower solidification rates), less segregation and smaller protrusion on the solidification front.^[108] The dendrite arm spacing, cross-flow velocity ^[235] and the surface tension have big effects on the entrapment of inclusions, related to the phenomena of pushing, engulfment or entrapment. ^[234-236] **Figure 40** shows how the secondary dendrite arm spacing increases with time and distance from the surface of an ESR ingot. ^[230]

Two studies ^[14, 237] of top-poured ingots found larger slag inclusions concentrate in the central bottom portion of the ingot, and in the outer portions of the ingot top, as shown in **figure 41** ^[14]. In bottom-poured ingots, the large inclusions were more uniformly distributed, and fewer in number. ^[14] The effect of teeming temperature on the distribution of large alumina inclusion clusters (larger than 50 μm) in an ingot is shown in **figure 42** ^[108]. This figure indicates that increased teeming temperature decreases the amount of inclusions, because it facilitates their floatation removal by natural convection.. Natural convection due to cooling the steel near the of the mold walls causes a downward flow along the walls and an upward flow in the middle of the ingot. The slow

solidification gives inclusions more time to collide, and the upward flow in the middle of the ingot promotes the separation of the inclusions to the top part of the ingot where they can be assimilated into the mold flux. In ingot A poured at a low temperature, the inclusions are trapped in the surface layer of the sides near the top of the ingot and in the central core at the bottom. In ingot B, the higher pouring temperature allowed more inclusions to escape to the top surface slag layer.^[108] For a bottom-poured 2t ingot (with taper) of 0.50% C, Al-Si-Killed steel, the high-melting-point inclusions (high alumina) predominate at the bottom of the ingot, while low-melting-point inclusions (sulphide and silicates) are more abundant in its top central portion, due to the mechanism of positive segregation.^[160] The shape and position of the bottom cone of negative segregation coincides with the bottom cone of inclusions in 2.2t bottom-poured ingots. This is attributed to these inclusions being entrapped in the dendrites of relatively pure equiaxed grains, and dropping to the bottom together as a shower.^[138] This hypothesis is supported by many researchers [227, 238-241].

Inclusion content is also related to yield in ingot casting. Exothermic “hot” top and/or an insulating powder in the ingot mold helps to extend the liquid stage near the mold top. This allows more inclusions to float into the top region before final solidification. To be effective, an optimal portion of the top part of the ingot, including the rough surface caused by the hot-top boards, must be cut off and not used in making the final rolled products. Sometimes, the part of the bottom is cut off as well. This removes the most inclusion rich regions from the finished product, at the expense of lower yield.

VI. SUMMARY AND RECOMMENDATIONS

This paper extensively reviews published research on inclusions in ingot steel and defects on ingot products, methods to measure and detect inclusions in steel, the causes of exogenous inclusions, and the transport and entrapment of inclusions during fluid flow, segregation and solidification of steel cast in ingot molds. Exogenous inclusions in ingots originate mainly from reoxidation of the molten steel, slag entrapment and lining erosion. The following methods can be used to minimize inclusions from entering the ingot mold and becoming entrapped during bottom-poured ingot casting:

- Minimize refractory erosion by optimizing steelmaking and steel refining:
 - fully deoxidize the steel (to lower dissolved oxygen levels) and avoid high-Mn-steels;

- minimize reoxidation materials (MnO and FeO) from slag carry-over;
- use pure refractories with minimal silica;
- design runners to minimize flow impact and velocity across on sensitive refractories;
- Avoid air reoxidation, especially during transfer operations, by using optimized flow conditions and effective sealing systems that include inert-gas shrouding.
- Optimize ingot geometry and negative taper to encourage inclusion floating and lessen turbulence and entrapment.
- Increase superheat entering the mold and optimize filling rates to avoid spouting.
- Use ceramic foam filters at the runner system near the ingate. ^[1-4]
- Use board top compounds to prolong surface solidification time, and lessen slag entrainment. ^[5] When using powder bags, suspend them near the bottom, but just above the “spout” height.
- Reheat ingots using temperature-time cycles that avoid precipitation of inclusions. ^[6]

Based on the knowledge gained from this review, the following four new methods are proposed for further investigation to improve steel cleanliness for bottom-poured ingot casting:

- Optimize the runner shape to absorb inclusions before they enter the mold. Inclusions tend to move upward so might be trapped by weirs or inclusion-entrapment cavities near the end of runners.
- Optimize ingate geometry design. Extend the ingate length to obtain a uniform vertical inflow into the mold, and control the velocity to decrease the top surface level fluctuations, turbulence, slag entrapment and reoxidation during filling. ^[7]
- Optimize teeming rate for a given ingate design to avoid “spouting” and turbulence. It is recommended that during the first several minutes, the teeming rate is kept at this low critical value, and then after there is some height of molten steel in the mold, the teeming rate can be increased gradually.
- Optimize the suspended height of powder bags close to the ingot bottom, or prevent spouting by adding a thin steel plate near the bottom of the mold, with powder on top .

Captions

| | |
|------------------|---|
| Table I. | Typical steel cleanliness requirements reported for various steel grades |
| Table II | Sources of macroinclusions in ingot steel ^[75] |
| Table III | Frequency of large exogenous inclusions in slab and plate detected by image scanning (No./cm ²) ^[14] |
| Table IV | Tracer oxides studies to identify exogenous inclusions sources: |
| Table V | The sizes and relative average volumes of various inclusion types : ^[51] |
| Table VI | Fluid flow investigation during mold filling process by different researchers |

Fig.1 Production of crude steel ingots in USA and in the world^[8]

Fig.2 Schematic of steelmaking process (left: Ovako Steel AB, Hofors, Sweden^[11]) and ingot bottom teeming process (right:^[10])

Fig. 3 Effect of inclusions on creation and linking of voids during deformation^[13]

Fig. 4 Comparison between experimental (dots) and predicted fatigue limit (curve) for different inclusion sizes at different strength levels.^[16]

Fig. 5 Effect of oxide-inclusion content on fatigue life of bearing steels (lifetime defined as revolutions until fatigue flaking of the surfaces of inner and outer rings or steel balls)^[20]

Fig.6 Morphology of alumina inclusions generated during deoxidation of low carbon Al-killed steels (a: Dendritic and clustered alumina^[39]; b: alumina cluster^[61]; c: coral-like alumina^[39])

Fig.7 Influence of temperature on size and neck-growth of the constituent particles of alumina clusters in induction-stirred baths, sampling 20 sec after Al-deoxidation in a 20kg LCAK steel ingot (induction stirred crucible)^[41]

Fig. 8 Alumina inclusions formed during the deoxidation of LCAK steel (a: flower-like plate alumina; b: aggregation of small polyhedral particles)^[49]

Fig. 9 Agglomeration of silica inclusions in a 80kg ingot^[52]

Fig.10 Typical sulfide inclusion (MnS) in steel ingot^[61]

Fig. 11 SEM and TEM analysis of AlN inclusions in high-Al ingot ((a)(a') plate-like, (b) (b') feathery, (c)(c') branched rod-like).^[54]

Fig. 12 Inclusion removal in the ladle after 3% additions of different deoxidizing metals^[62]

Fig.13 Size distribution of inclusions in ingots measured by Franklin ^[63], Zhang et al ^[61] and Miki et al ^[52]

Fig.14 Typical slag inclusions in steel ingot (a: calcium-alumina silicate) ^[50], b: either alumina silicate or a mixed oxide phase ^[50], c: Crystals of alumina on the surface of a globular slag inclusion ^[53], d: Globular inclusions of aluminosilicate with impregnated magnesium spinel ^[53])

Fig.15 Typical exogenous inclusions in steel (a: inclusions from lining refractory ^[40], b: exogenous inclusion in C-Mn large forging (200 ton), 34%MnO-28% Al_2O_3 -38% SiO_2 ^[75], c: Al_2O_3 58.35%, SiO_2 27.57%, CaO 9.43%, Cr_2O_3 3.34%, FeO 1.32% ^[61]

Fig.16 Inclusion clusters in Al-killed steel

Fig. 17 Sizes of inclusions during teeming ^[51]

Fig. 18 A slag spot defect on a cold-rolled sheet ^[73]

Fig. 19 Line shell defects on stainless flat-rolled product from ingot ^[75]

Fig. 20 Example of tunnel or lap defect on rolled plate due to pickled-out silicate inclusions ^[75]

Fig. 21 Defects on surface of steel strip rolled from ingot steel: (a) Sliver (b,c) Blisters and (d) Pipe lamination ^[67]

Fig.22 Inclusions outlining the former surface of bubbles captured in ingot steel (left) ^[61] and in continuous cast steel (right) ^[79])

Fig. 23 The formation of inclusions in steels deoxidized with aluminum (based on Hilty^[21])

Fig. 24 Devices for stream protection from air absorption ^[152]

Fig. 25 Effect of argon sealing on alumina content and number of large inclusions in ingot ^[7]

Fig. 26 Ternary composition of casting-pit refractories, altered refractories, and scums for bottom-teeming carbon steel ^[161]

Fig. 27 Schematic of bottom pouring showing entrapment of powder added to mold bottom in bag ^[170]

Fig. 28 Effect of upgate design on the fluid flow pattern into the ingot mold bottom during bottom teeming process (left: upgate with taper; right: upgate without taper) ^[173]

Fig.29 Effect of teeming rate on the free surface of steel entering a bottom-poured 8-inch ingot mold (left: 11.5 inch/min in ingot, right: 503.2 inch/min in ingot) ^[175]

Fig. 30 Effect of brick materials on wear rate (high manganese steel) ^[7]

Fig. 31 Ternary composition of manganese aluminosilicate ($\text{MnO-Al}_2\text{O}_3\text{-SiO}_2$ system) found in forgings, ladle glaze analysis, reaction layers formed between refractory and liquid steel ^[75]

Fig. 32 Microstructure of the refractory/steel interface in a bottom-pour runner sample from K1040-type steel (unetched, white regions are metal prills ^[64] (A: Na₂O 0.5%, MgO 0.8%, Al₂O₃ 66.5%, SiO₂ 21.1%, K₂O 2.1%, CaO 0.2%, TiO₂ 0.5%, MnO 7.2%, FeO 1.3%; B: (primary matrix) Na₂O 0.3%, MgO 1%, Al₂O₃ 35.7%, SiO₂ 54.2%, K₂O 2.9%, CaO 0.2%, TiO₂ 1%, MnO 3.2%, FeO 1.5%)

Fig. 33 Ladle sand buildup block ^[73]

Fig.34 Defect from runner erosion ^[51] (a: Group of silicates from feeder-head titles in rolled billet; b: Increase of maximum size of eroded silicates during teeming)

Fig. 35 Effect of the angle of contact, radius, and pressure on the strength of two solid particles immersed in liquid steel ^[23]

Fig. 36 Dendritic inclusions formed from a spherical primary silica in Fe-10%Ni alloy deoxidized with silicon (inclusions in ingot ^[189])

Fig.37 Alumina clogs at the submerged entry nozzle during continuous casting of low carbon Al-killed steel (a: Alumina inclusions clogged ^[39], b: Dendritic cluster and plate-like clusters clogs ^[40])

Fig. 38 Simulated fluid flow at 800s and macrosegregation at 3800s (numbers indicate carbon concentration in mass %) in a Fe-0.19%C ingot ^[218]

Fig. 39 Comparison of solidification pattern of a conventional melting furnace and ESR ^[230]

Fig. 40 Secondary dendrite arm spacing measured in 1800mm ϕ ESR ingot ^[230]

Fig. 41 Distribution of large slag inclusions in a top-poured 5 t ingot ^[14]

Fig. 42 Distribution of large inclusions in bottom-poured ingots at different teeming temperatures ^[108]

Table I. Typical steel cleanliness requirements reported for various steel grades

| Steel product | Maximum impurity fraction | Maximum inclusion size |
|---------------------------------|--|--|
| Automotive & deep-drawing Sheet | [C]≤30ppm, [N]≤30ppm ^[242] | 100μm ^[242, 243] |
| Drawn and Ironed cans | [C]≤30ppm, [N]≤30ppm, T.O.≤20ppm ^[242] | 20μm ^[242] |
| Line pipe | [S]≤30ppm ^[244] , [N]≤35ppm, T.O.≤30ppm ^[245] , [N]≤50ppm ^[246] | 100μm ^[242] |
| Ball Bearings | T.O.≤10ppm ^[97, 244] | 15μm ^[97, 245] |
| Tire cord | [H]≤2ppm, [N]≤40ppm, T.O.≤15ppm ^[245] | 10μm ^[245] 20μm ^[243] |
| Heavy plate steel | [H]≤2ppm, [N]30-40ppm, T.O.≤20ppm ^[245] | Single inclusion 13μm ^[242] Cluster 200μm ^[242] |
| Wire | [N]≤60ppm, T.O.≤30ppm ^[245] | 20μm ^[245] |

Table II Sources of macroinclusions in ingot steel^[75]

| Source | Approximate frequency of occurrence, % |
|-----------------------------------|--|
| Attack or fluxing of refractories | 58 |
| High-alumina refractories | 15 |
| Deoxidation products | 15 |
| Slag | 8 |
| Slag+deoxidation products | 4 |

Table III Frequency of large exogenous inclusions in slab and plate detected by image scanning (No./cm²)^[14]

| Plate scanning investigation | | | | Slab scanning investigation | | | |
|------------------------------|-----------|------------|----------|-------------------------------|----------------------------|-----------|----------|
| 100-250μm | 251-500μm | 501-1000μm | 1000μm | 30-50μm | 51-100μm | 101-250μm | >250μm |
| 5-10 sulphide 5-15 oxides | 2-7oxide | 2-5oxide | 1-3oxide | 10-15 sulphide 10-20 oxide | 1-3 sulphide 8-14 oxide | 4-7oxide | 1-3oxide |

Table IV Tracer oxides studies to identify exogenous inclusions sources:

| Researchers | Description | Year | Ref. |
|-----------------|---|------|-------|
| Mori et al | La ₂ O ₃ oxide added to steelmaking furnace slag | 1965 | [247] |
| Middleton et al | Cerium oxide (CeO ₂) to sand Furnace slag: Ba Ladle refractory: Zr, and Ba Nozzle sleeves: Ba | 1967 | [140] |
| Ichinoe et al | La was plugged into aluminum to be added in the mould | 1970 | [108] |
| Benko et al | Ba was added into slag and lining | 1972 | [141] |
| Zeder and Pocze | La to ladle lining, Yb to stopper-rod in ladle, Sm to trumpet bricks, Eu to spider bricks, Ho to runner bricks. | 1980 | [142] |
| Komai et al | SrO to tundish slag for the continuous casting of low carbon Al-killed steel | 1981 | [143] |
| Byrne et al | Barium oxide (BaO) added to the ladle slag Cerium oxide (CeO ₂) added to the tundish slag Strontium oxide (SrO ₂) added to the mold slag | 1985 | [70] |
| Byrne and Cramb | Cerium oxide (CeO ₂) added to the ladle shroud cell and the tundish slag | 1988 | [76] |
| Burty et al | La was added into steel during RHOB after Al-killing, then 5 minutes stirring, to evaluate reoxidation, understand clogging at SEN, and inclusion floating to top slag. | 1994 | [144] |
| Zhang and Cai | BaCO ₃ to ladle slag, SrCO ₃ to tundish slag, La ₂ O ₃ to mold slag for CC production of LCAK steel. | 1995 | [145] |
| Zhang and Cai | La ₂ O ₃ to ingot mold powder. 17 of 28 analyzed <u>slag</u> inclusions had the composition of mold powder. | 1996 | [146] |
| Rocabois et al | La was added into steel during steel refining after Al-killing to study the origin of slivers defects | 2003 | [77] |

Table V The sizes and relative average volumes of various inclusion types : ^[51]

| Type of inclusions | Diameter (μm) | Relative volume |
|---|---------------|-----------------|
| Alumina, spinel, and $\text{CaO} \cdot 6\text{Al}_2\text{O}_3$ (other than cluster) | 5 | 1 |
| Other calcium aluminates | 27 | ~160 |
| Secondary deoxidation products (Si-Killed steel) | 32 | ~260 |
| Primary deoxidation products (Si-Killed steel) | 49 | ~940 |
| Erosion silicates (Al-killed Steel) | 64 | ~2100 |
| Erosion Silicates (Si-killed Steel) | 107 | ~9800 |

Table VI Fluid flow investigation during mold filling process by different researchers

| Author | Main content | Year | Ref. |
|----------------------|---|---------------|--------------------|
| Van Der Graaf et al. | Snapshots and free surface pattern of filling process of iron and aluminum in a plate cavity; Water model study (PIV measurement) 3D Fluid flow simulation of water by Flow-3D (VOF model for moving free surface modeling) | 2001 | [248] |
| Hong et al. | 3D Fluid flow simulation (VOF model for moving free surface modeling) | 2001 | [249] |
| Lin | 2D Fluid flow, heat transfer and solidification simulation (VOF model for moving free surface modeling) | 1999 | [250] |
| Yuan et al | 3D Fluid flow, heat transfer and solidification simulation (VOF model for moving free surface modeling) and temperature measurement in thin plate filling process | 1997 | [251] |
| Xu | 2D Fluid flow, heat transfer (VOF model for moving free surface modeling) and visualization of flow pattern in a water model of a thin plate filling process | 1994, 1996 | [214] [212] |
| Xue et al | 3D Fluid flow simulation (VOF model for moving free surface modeling) and visualization of flow pattern in a water model of plate-like square ingot filling process | 1993 | [252] |
| Xue et al | Water model study of flow pattern, particle motion in a plate-like ingot filling process with different gate designs | 1993 | [253] |
| Jong et al | Measurement of flow pattern for plate ingot or large square ingot filling process | 1991 | [254] |
| Mishima and Szekely | 2D Fluid flow and heat transfer simulation (VOF model for moving free surface modeling) in mold filling of a round ingot | 1989 | [255] |
| Davidson et al | 2D flow transition in vacuum arc remelting | 2000 | [256] |
| R. Eriksson | 2D water model velocity measurement in ingot during bottom pouring process | 2001 | [105] |
| | 2D numerical simulation of fluid flow in bottom teeming ingot | 2004 | [172] |
| Zhang and Thomas | 3D fluid flow, inclusion motion, and free surface fluctuation during bottom teeming process of steel ingot | 2002- 2004 | [173, 175, 257] |

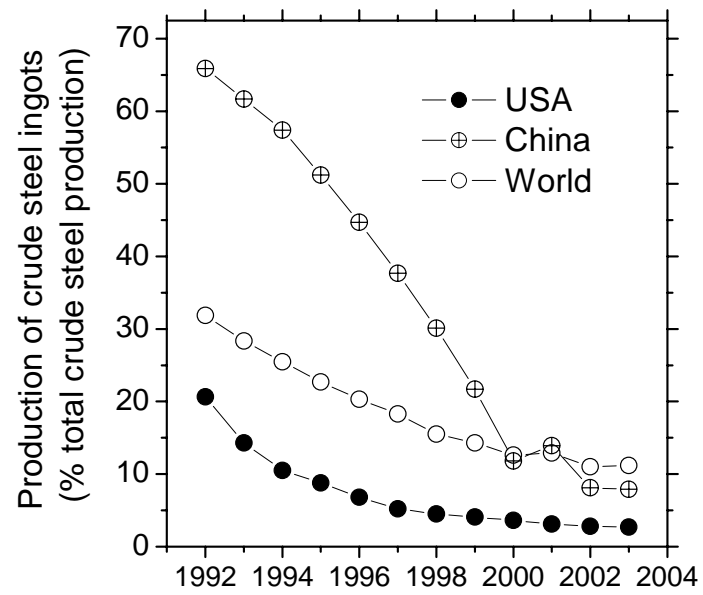


Fig.1 Production of crude steel ingots in USA and in the world ^[8]

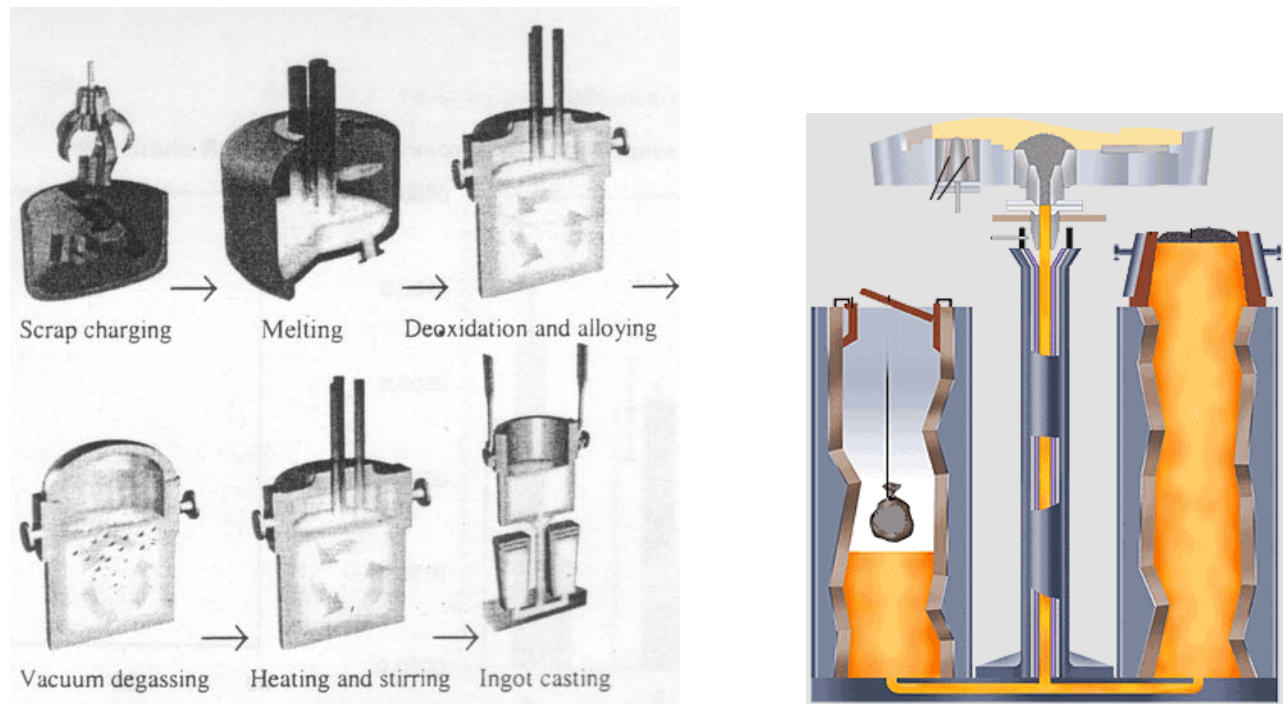


Fig.2 Schematic of steelmaking process (left: Ovako Steel AB, Hofors, Sweden ^[11]) and ingot bottom teeming process (right: ^[10])

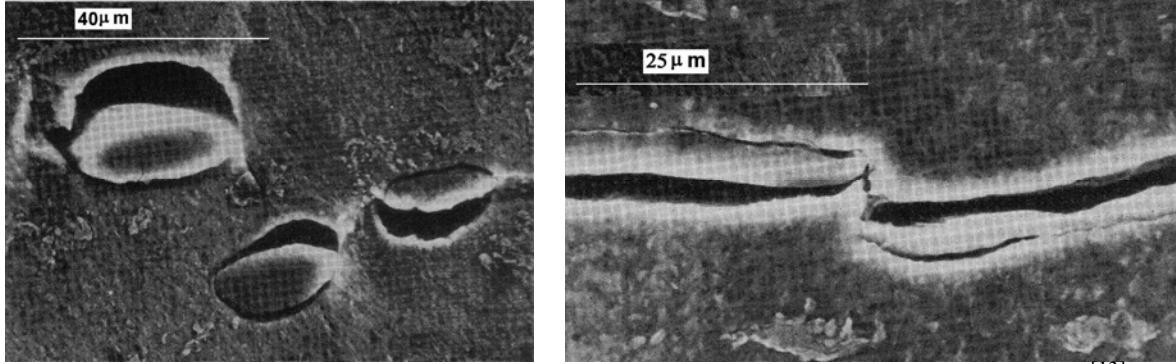


Fig. 3 Effect of inclusions on creation and linking of voids during deformation ^[13]

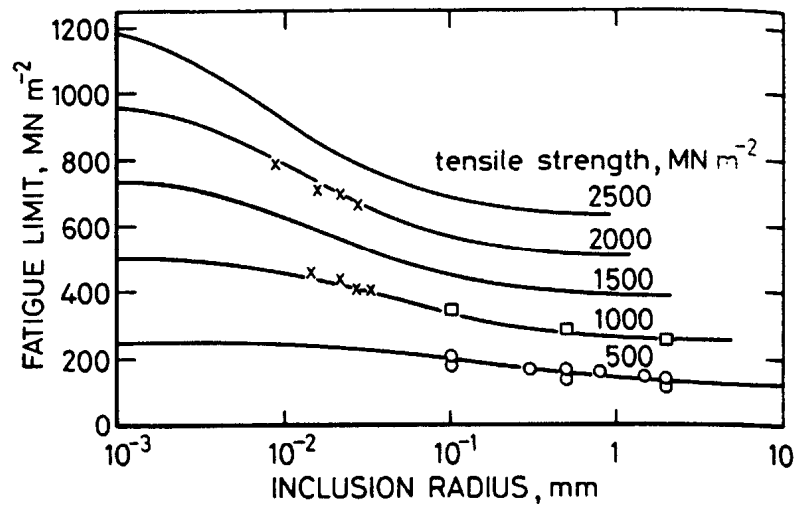


Fig. 4 Comparison between experimental (dots) and predicted fatigue limit (curve) for different inclusion sizes at different strength levels. ^[16]

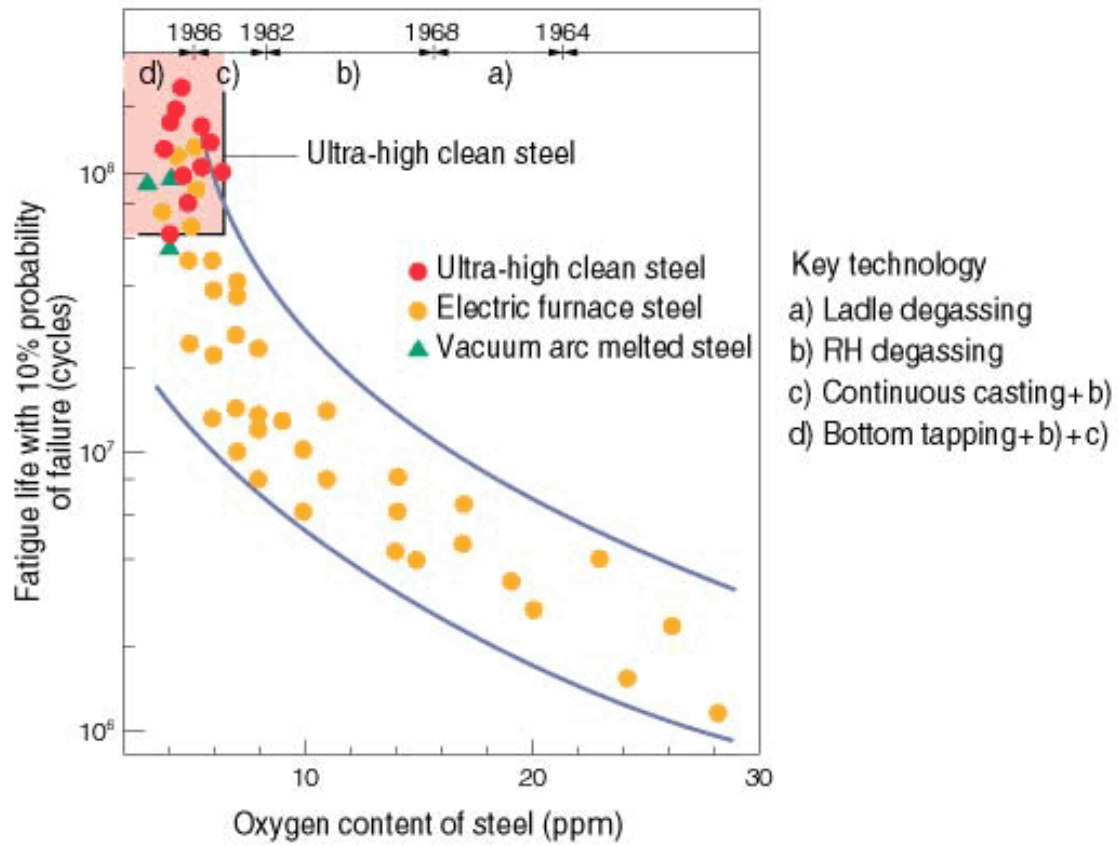


Fig. 5 Effect of oxide-inclusion content on fatigue life of bearing steels (lifetime defined as revolutions until fatigue flaking of the surfaces of inner and outer rings or steel balls) ^[20]

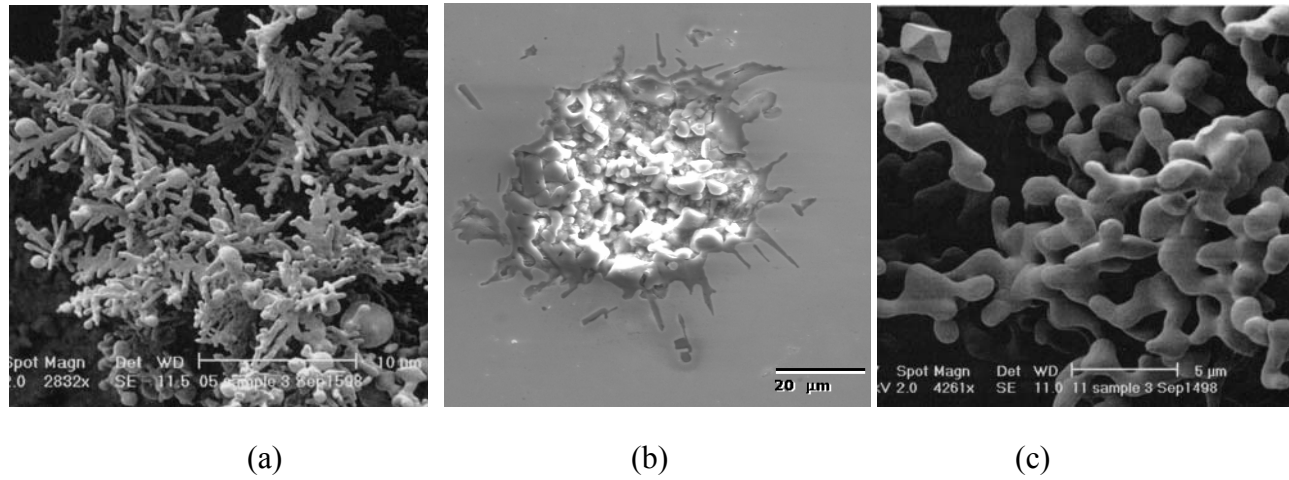


Fig.6 Morphology of alumina inclusions generated during deoxidation of low carbon Al-killed steels (a: Dendritic and clustered alumina ^[39]; b: alumina cluster ^[61]; c: coral-like alumina ^[39])

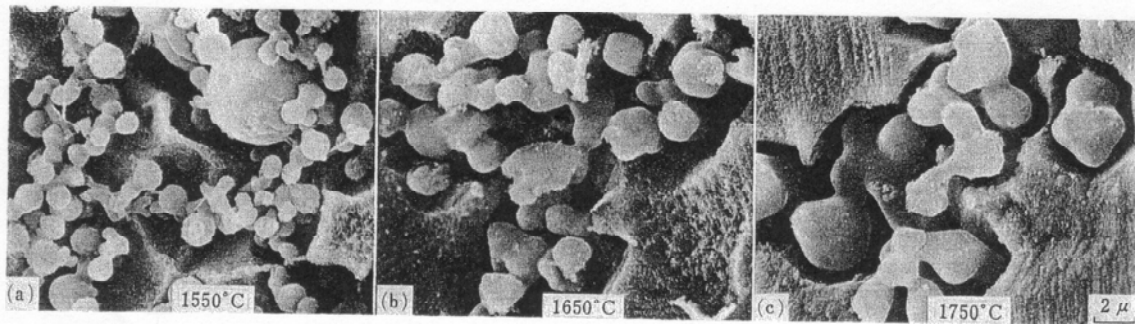
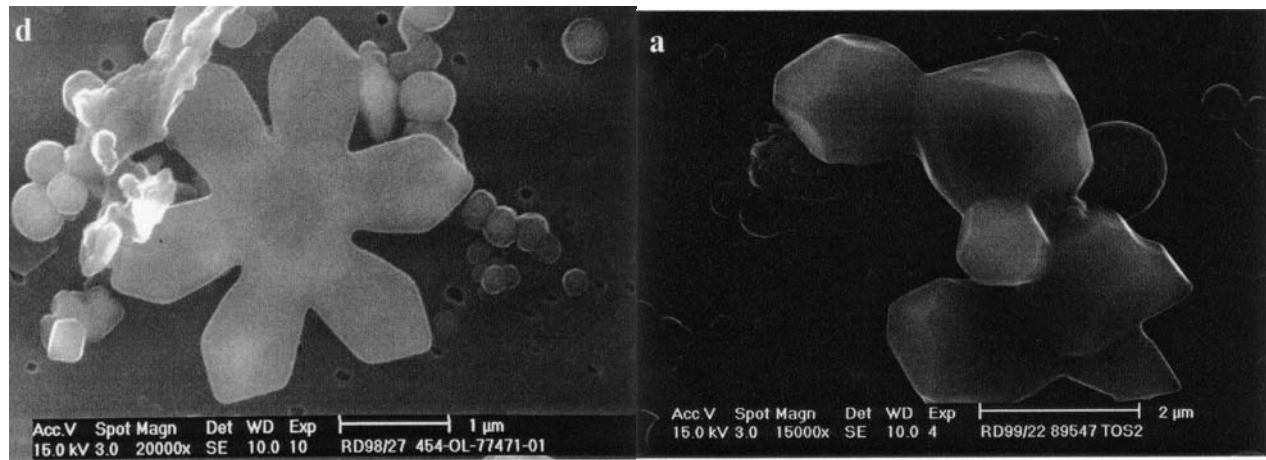


Fig.7 Influence of temperature on size and neck-growth of the constituent particles of alumina clusters in induction-stirred baths, sampling 20 sec after Al-deoxidation in a 20kg LCAK steel ingot (induction stirred crucible) ^[41]



(a)

(b)

Fig. 8 Alumina inclusions formed during the deoxidation of LCAK steel (a: flower-like plate alumina; b: aggregation of small polyhedral particles) ^[49]

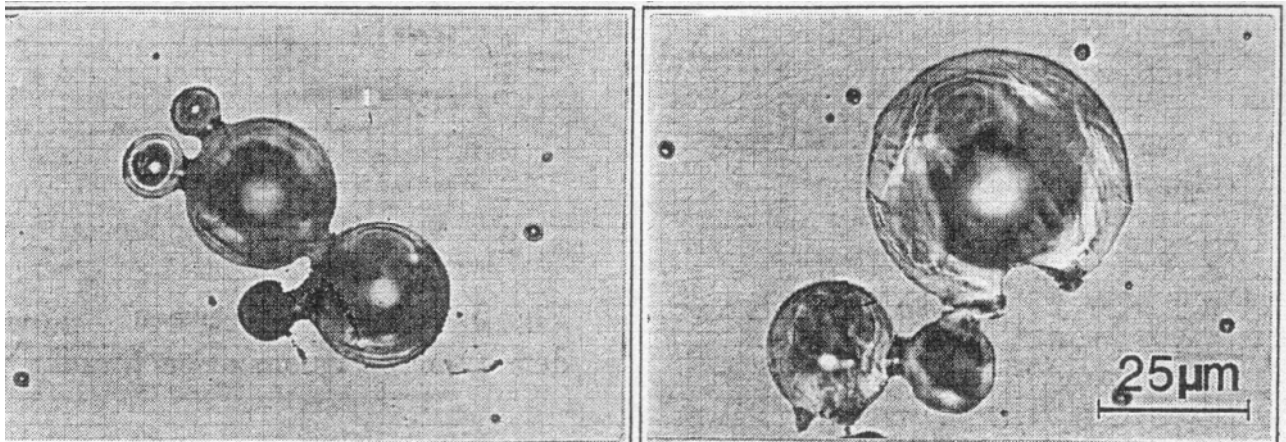


Fig. 9 Agglomeration of silica inclusions in a 80kg ingot ^[52]

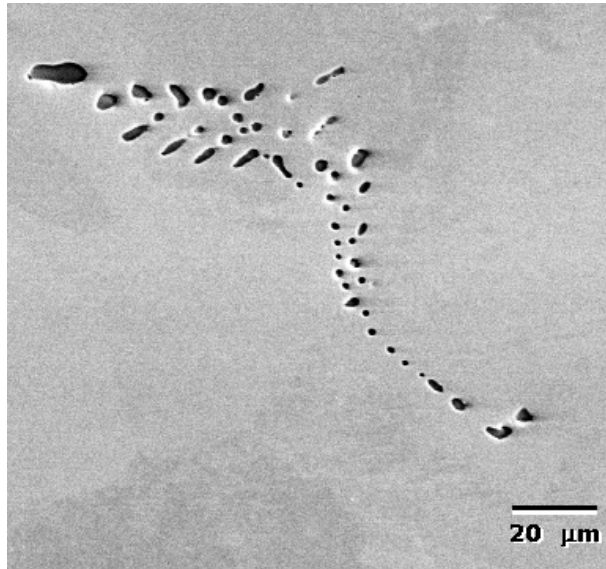


Fig.10 Typical sulfide inclusion (MnS) in steel ingot ^[61]

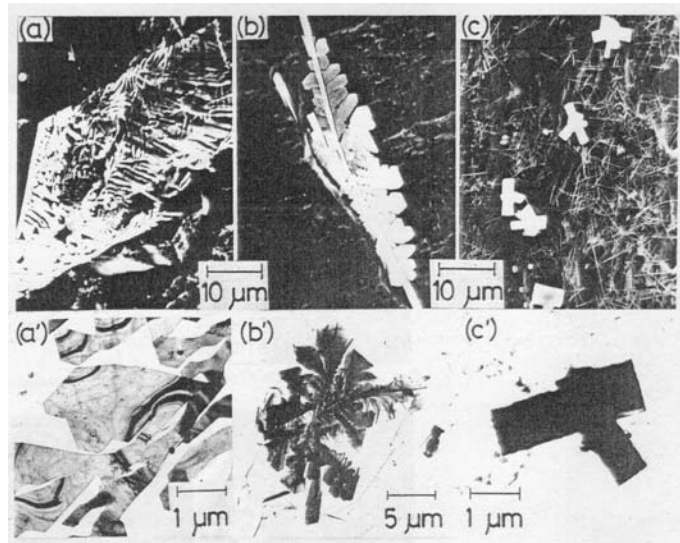


Fig. 11 SEM and TEM analysis of AlN inclusions in high-Al ingot ((a)(a') plate-like, (b) (b') feathery, (c)(c') branched rod-like).^[54]

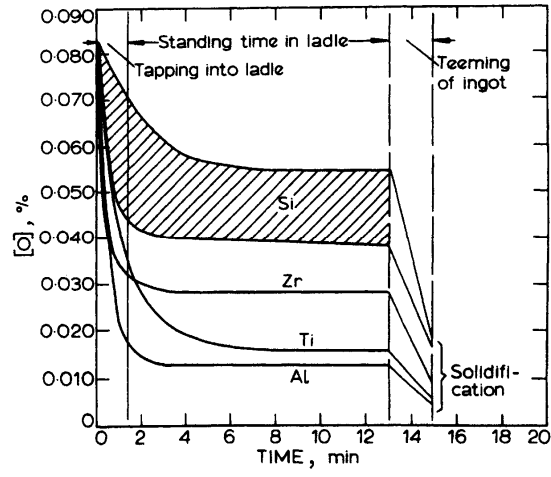


Fig. 12 Inclusion removal in the ladle after 3% additions of different deoxidizing metals ^[62]

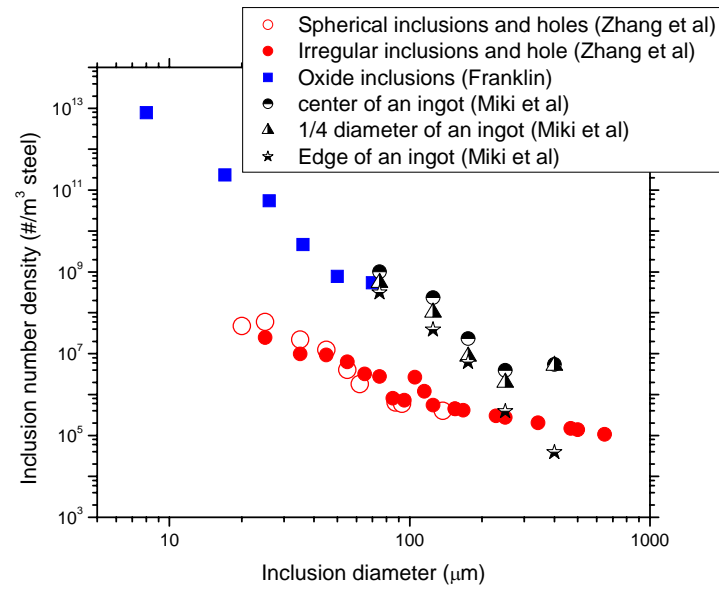


Fig.13 Size distribution of inclusions in ingots measured by Franklin^[63], Zhang et al^[61] and Miki et al^[52]

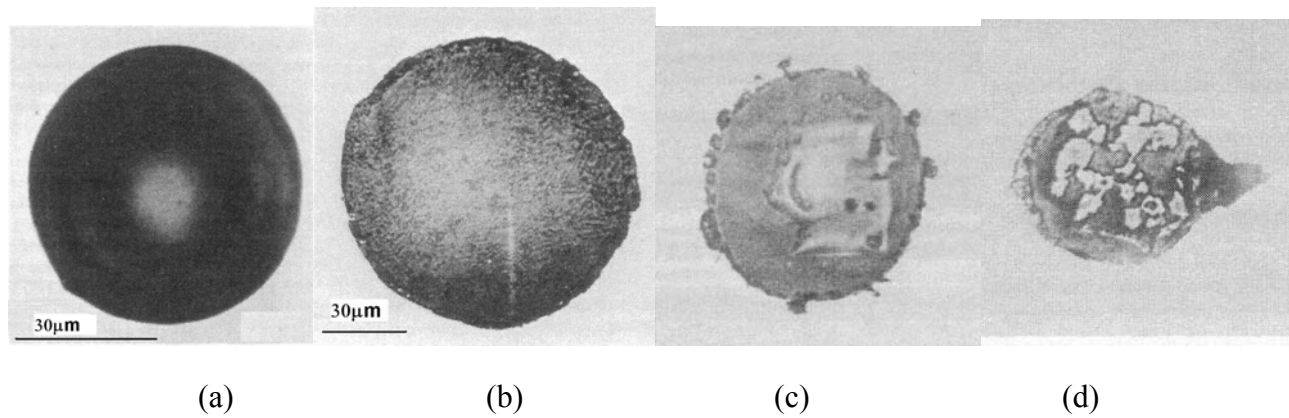


Fig.14 Typical slag inclusions in steel ingot (a: calcium-alumina silicate)^[50], b: either alumina silicate or a mixed oxide phase^[50], c: Crystals of alumina on the surface of a globular slag inclusion^[53], d: Globular inclusions of aluminosilicate with impregnated magnesium spinel^[53])

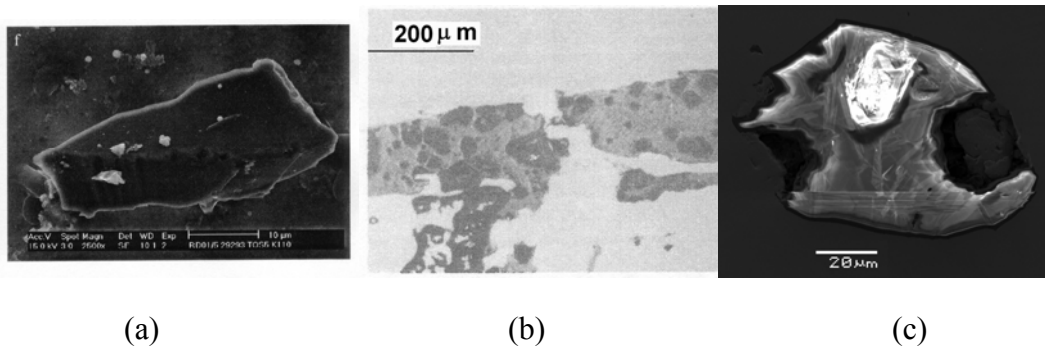
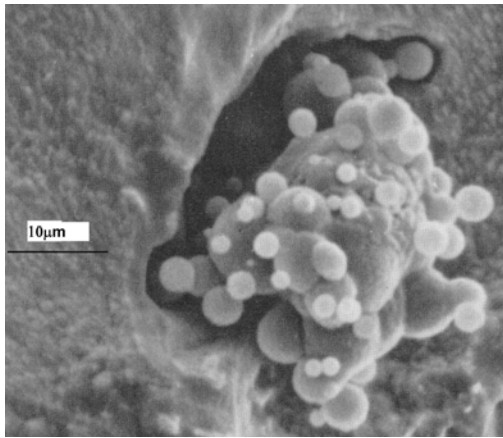
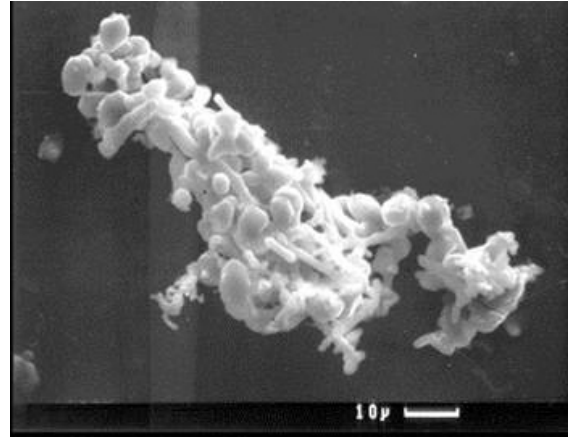


Fig.15 Typical exogenous inclusions in steel (a: inclusions from lining refractory^[40], b: exogenous inclusion in C-Mn large forging (200 ton), 34%MnO-28% Al₂O₃-38%SiO₂^[75], c: Al₂O₃ 58.35%, SiO₂ 27.57%, CaO 9.43%, Cr₂O₃ 3.34%, FeO 1.32%^[61]



(a) ^[65]



(b) ^[66]

Fig.16 Inclusion clusters in Al-killed steel

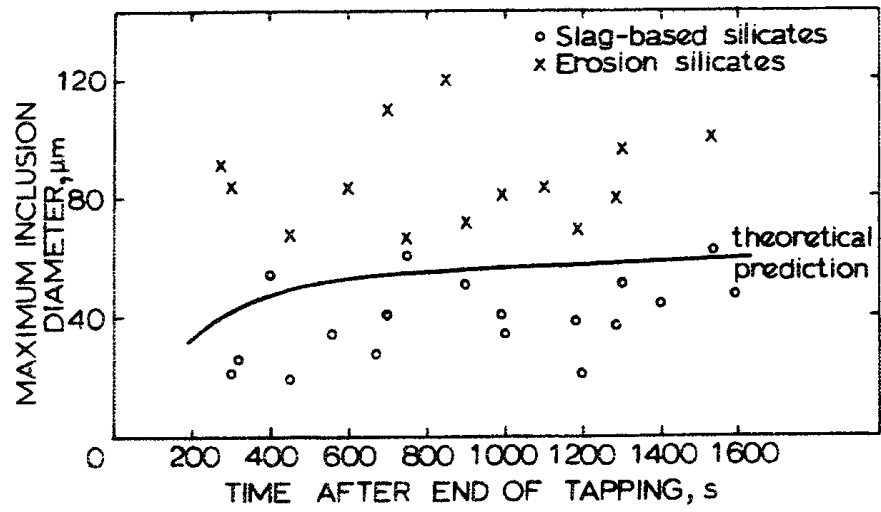


Fig. 17 Sizes of inclusions during teeming^[51]

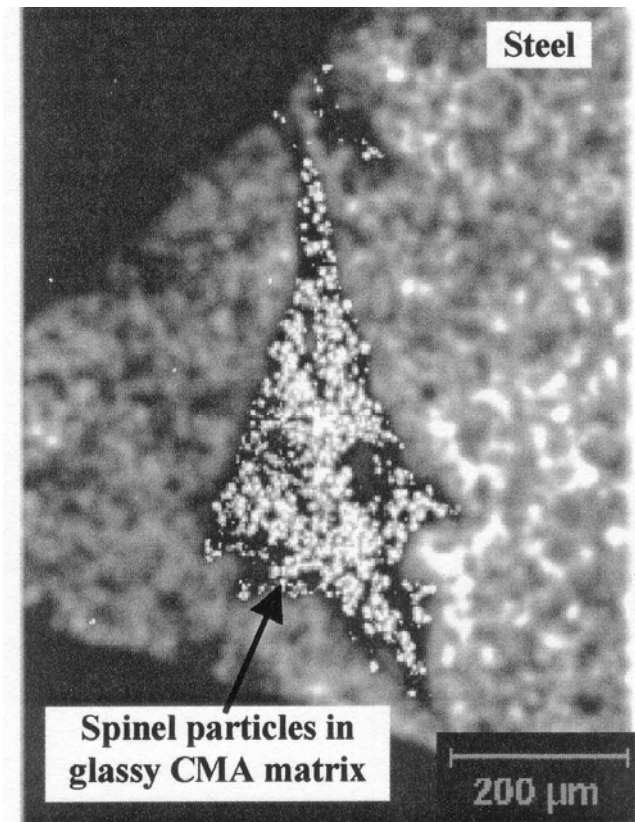
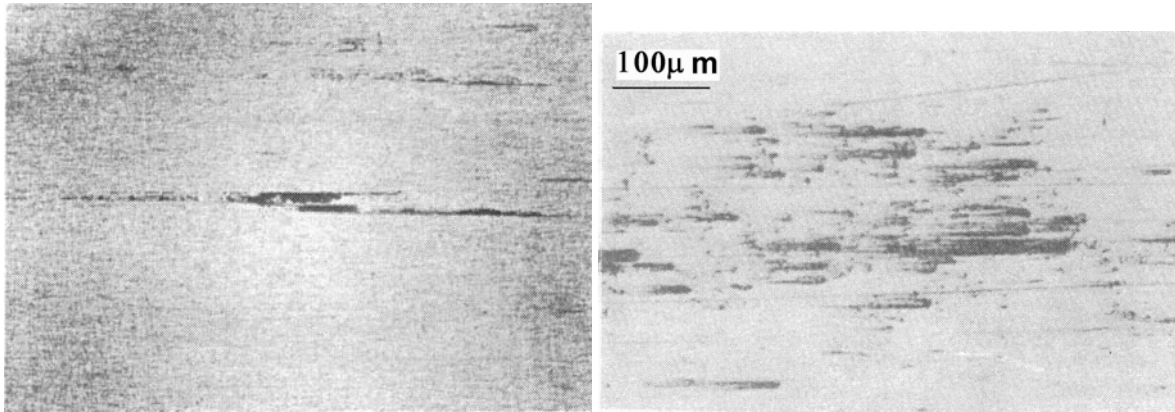


Fig. 18 A slag spot defect on a cold-rolled sheet ^[73]



(a) Line-shell defect

(b) Typical scratch marks due to hard inclusions

Fig. 19 Line shell defects on stainless flat-rolled product from ingot ^[75]

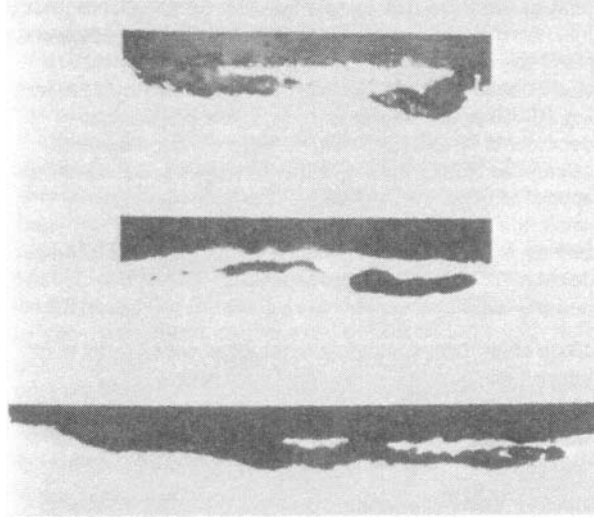


Fig. 20 Example of tunnel or lap defect on rolled plate due to pickled-out silicate inclusions ^[75]

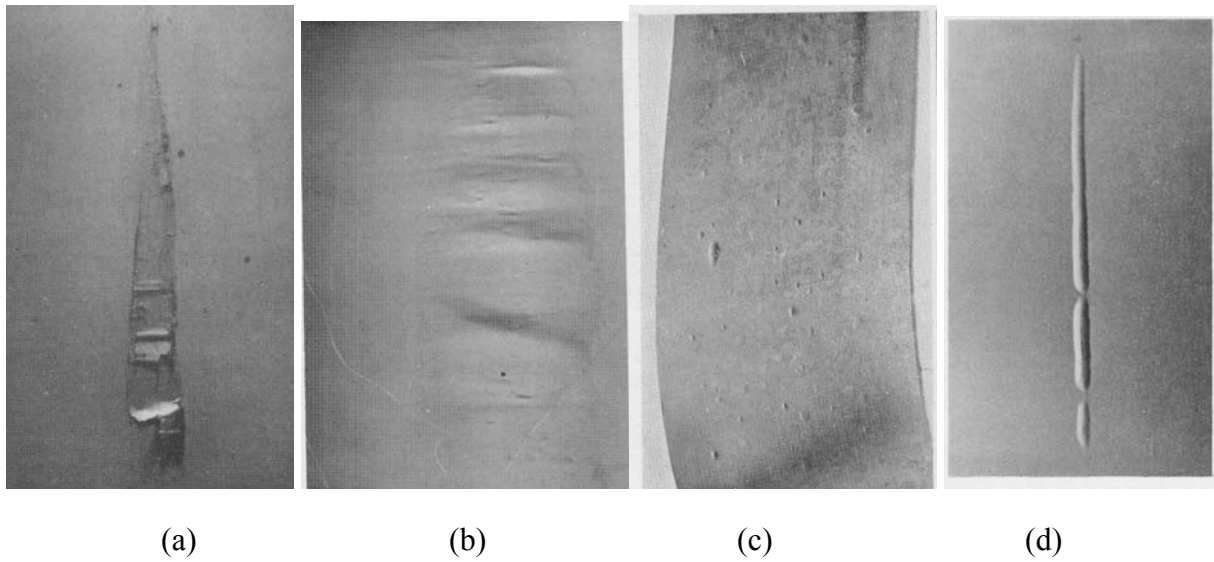


Fig. 21 Defects on surface of steel strip rolled from ingot steel: (a) Sliver (b,c) Blisters and (d) Pipe laminationon ^[67]

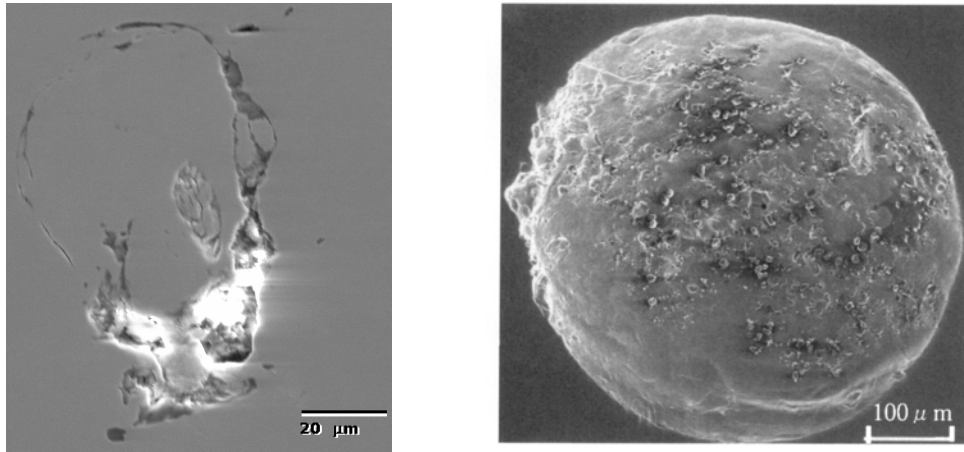


Fig.22 Inclusions outlining the former surface of bubbles captured in ingot steel (left) ^[61] and in continuous cast steel (right ^[79])

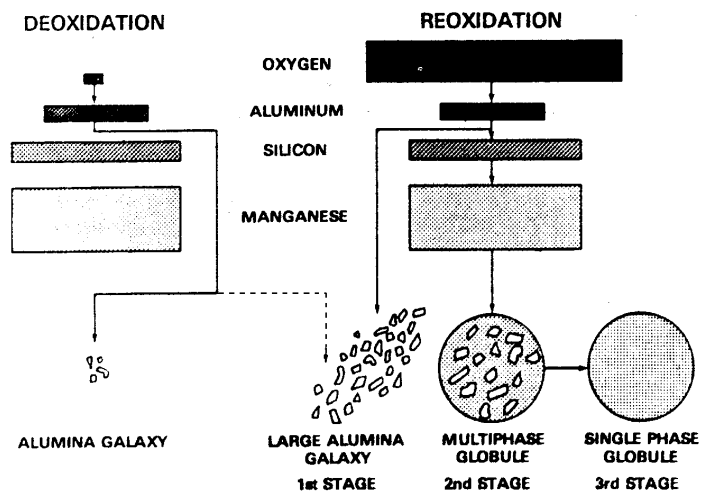


Fig. 23 The formation of inclusions in steels deoxidized with aluminum (based on Hilty^[21])

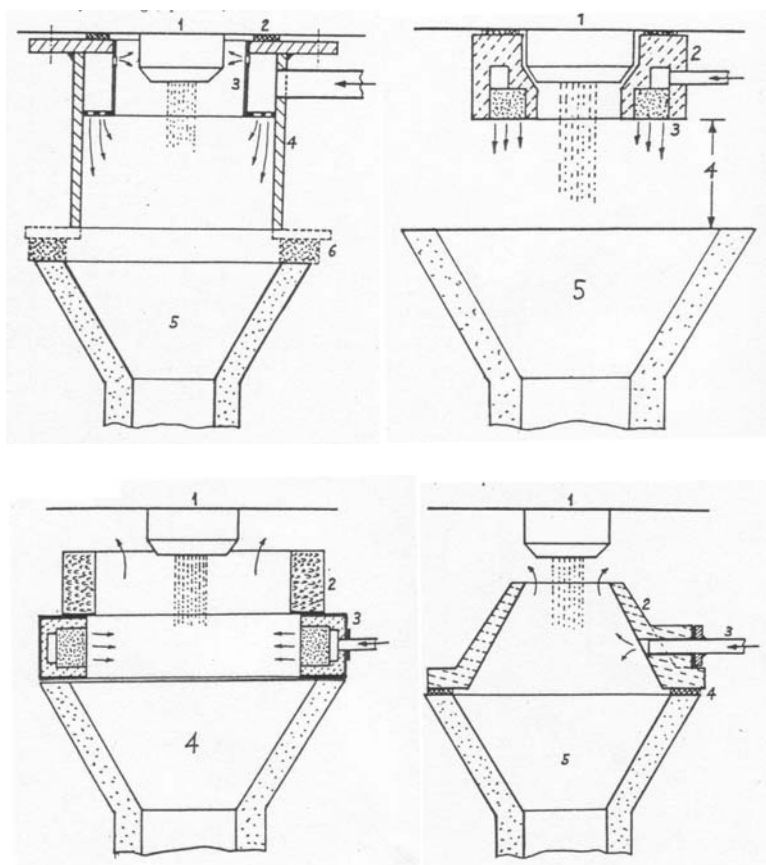


Fig. 24 Devices for stream protection from air absorption ^[152]

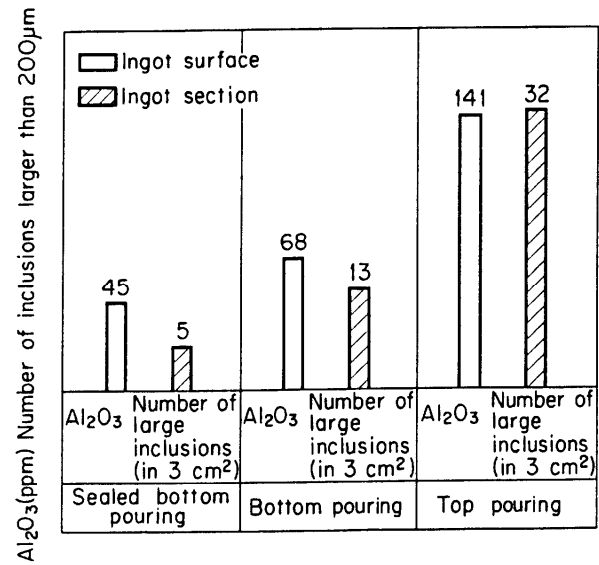


Fig. 25 Effect of argon sealing on alumina content and number of large inclusions in ingot ^[7]

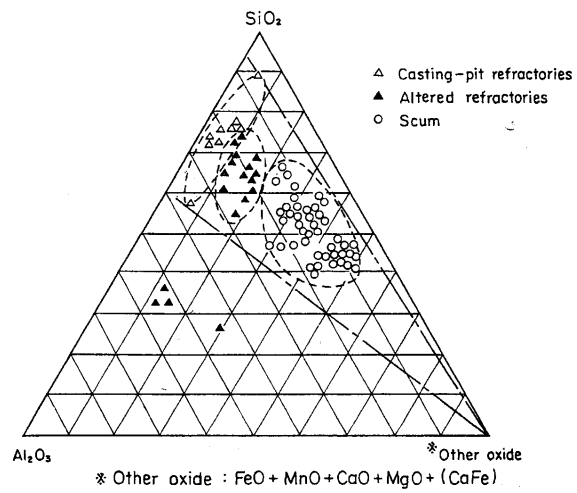


Fig. 26 Ternary composition of casting-pit refractories, altered refractories, and scums for bottom-teeming carbon steel ^[161]

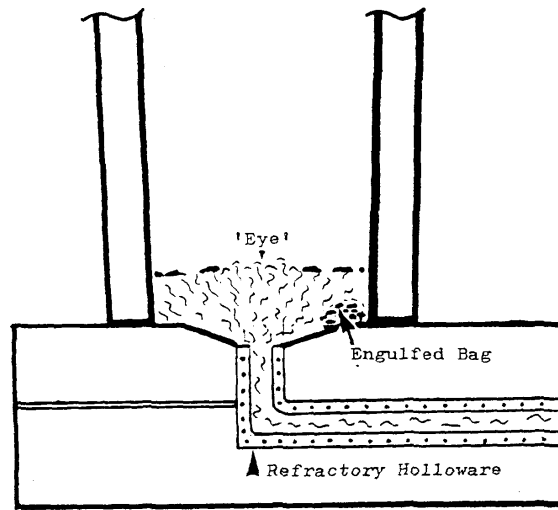


Fig. 27 Schematic of bottom pouring showing entrapment of powder added to mold bottom in bag
[170]

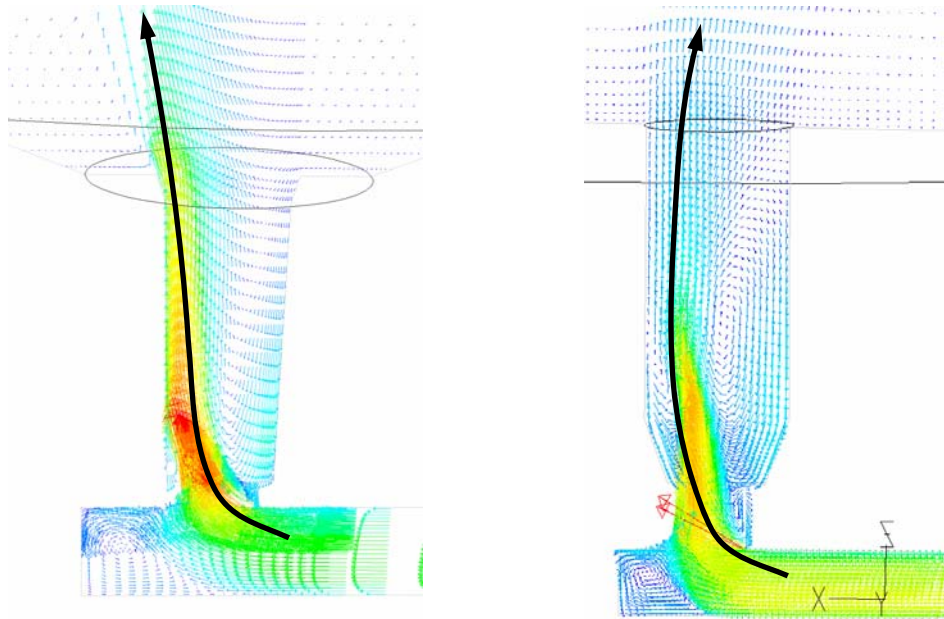


Fig. 28 Effect of upgate design on the fluid flow pattern into the ingot mold bottom during bottom teeming process (left: upgate with taper; right: upgate without taper) ^[173]

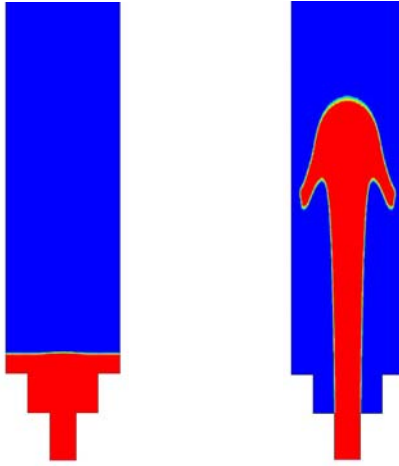
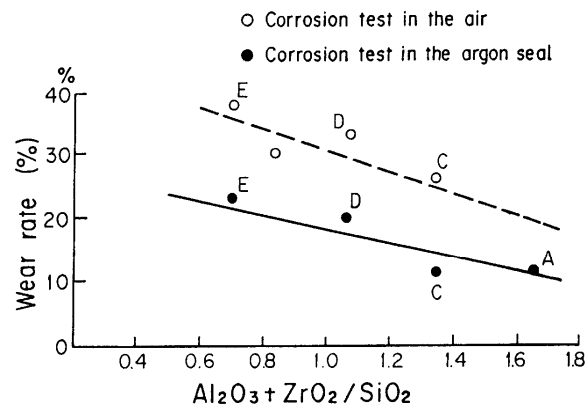


Fig.29 Effect of teeming rate on the free surface of steel entering a bottom-poured 8-inch ingot mold (left: 11.5 inch/min in ingot, right: 503.2 inch/min in ingot) ^[175]



| Material of brick | Chemical Composition(%) | | | Refracto-riness (SK) |
|----------------------|-------------------------|--------------------------------|------------------|----------------------|
| | SiO ₂ | Al ₂ O ₃ | ZrO ₂ | |
| A Mullite (burnt) | 36. ⁷ | 60. ⁰ | — | 36 ⁺ |
| B Chamotte (unburnt) | 48. ⁹ | 40. ⁶ | — | 33 ⁺ |
| C Semizircon (burnt) | 40. ⁷ | 13. ⁹ | 40. ⁶ | 34 |
| D Chamotte (burnt) | 45. ⁰ | 47. ² | — | 35 |
| E Chamotte (burnt) | 54. ⁹ | 38. ⁰ | — | 31 ⁺ |

Fig. 30 Effect of brick materials on wear rate (high manganese steel) ^[7]

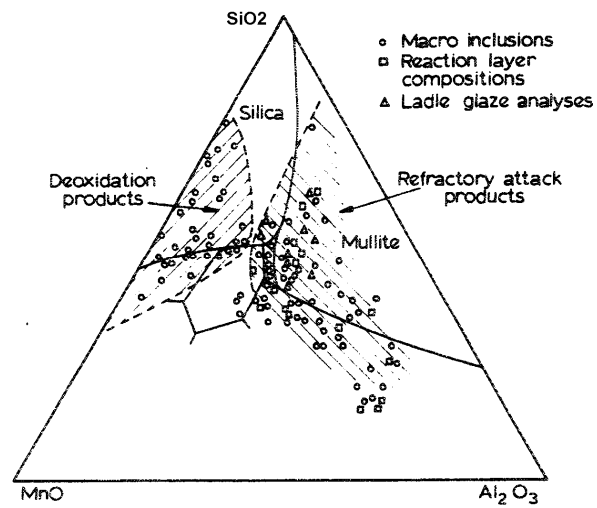


Fig. 31 Ternary composition of manganese aluminosilicate ($\text{MnO}-\text{Al}_2\text{O}_3-\text{SiO}_2$ system) found in forgings, ladle glaze analysis, reaction layers formed between refractory and liquid steel ^[75]

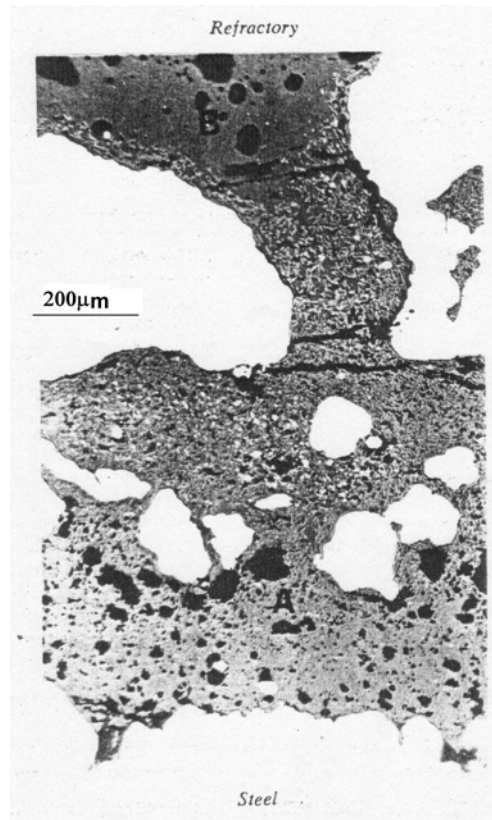


Fig. 32 Microstructure of the refractory/steel interface in a bottom-pour runner sample from K1040-type steel (unetched, white regions are metal prills^[64] (A: Na₂O 0.5%, MgO 0.8%, Al₂O₃ 66.5%, SiO₂ 21.1%, K₂O 2.1%, CaO 0.2%, TiO₂ 0.5%, MnO 7.2%, FeO 1.3%; B: (primary matrix) Na₂O 0.3%, MgO 1%, Al₂O₃ 35.7%, SiO₂ 54.2%, K₂O 2.9%, CaO 0.2%, TiO₂ 1%, MnO 3.2%, FeO 1.5%))

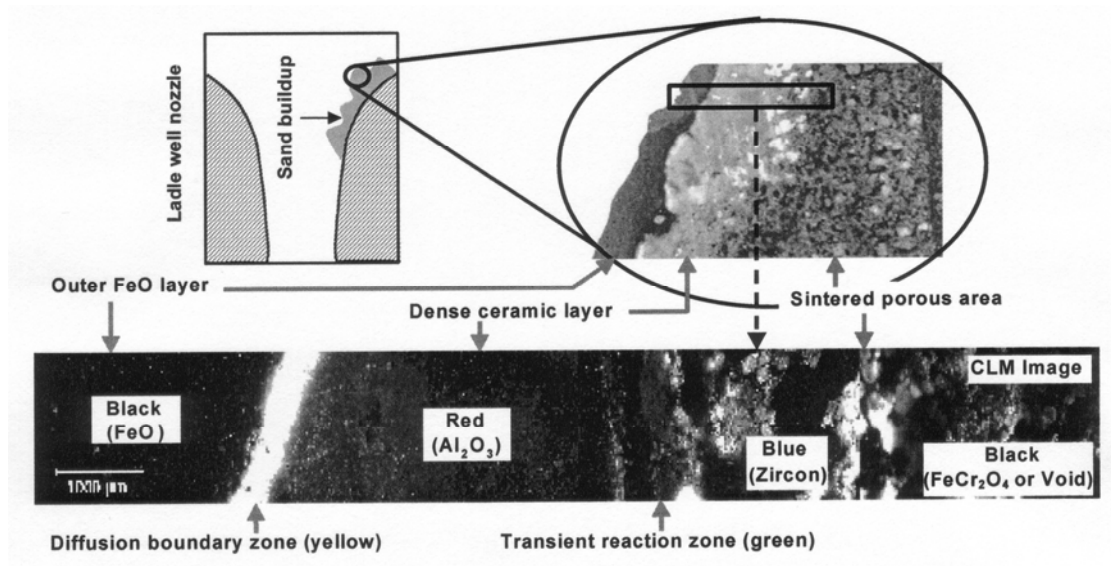


Fig. 33 Ladle sand buildup block^[73]

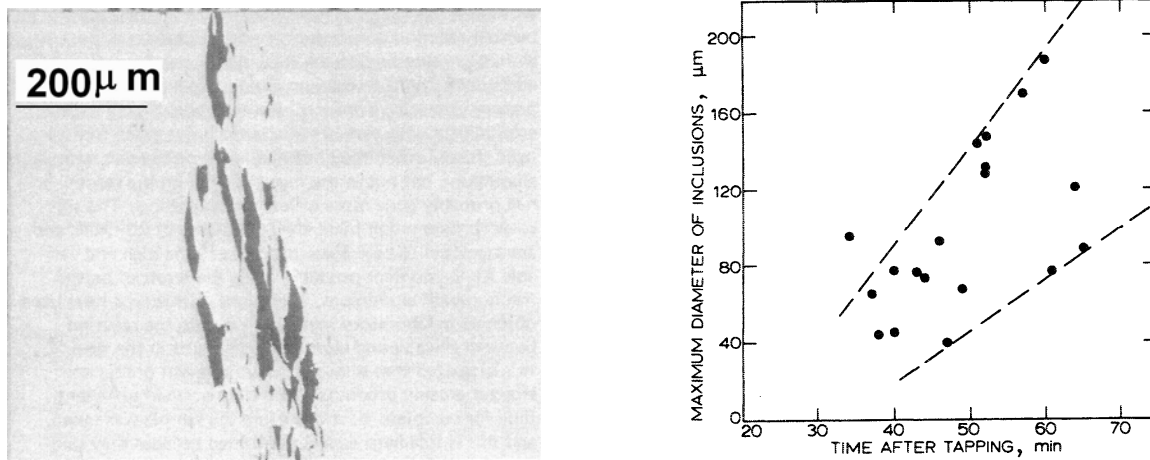


Fig.34 Defect from runner erosion^[51] (a: Group of silicates from feeder-head tiles in rolled billet;
b: Increase of maximum size of eroded silicates during teeming)

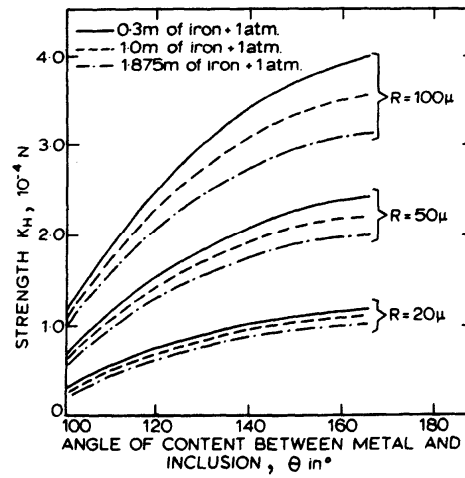


Fig. 35 Effect of the angle of contact, radius, and pressure on the strength of two solid particles immersed in liquid steel ^[23]

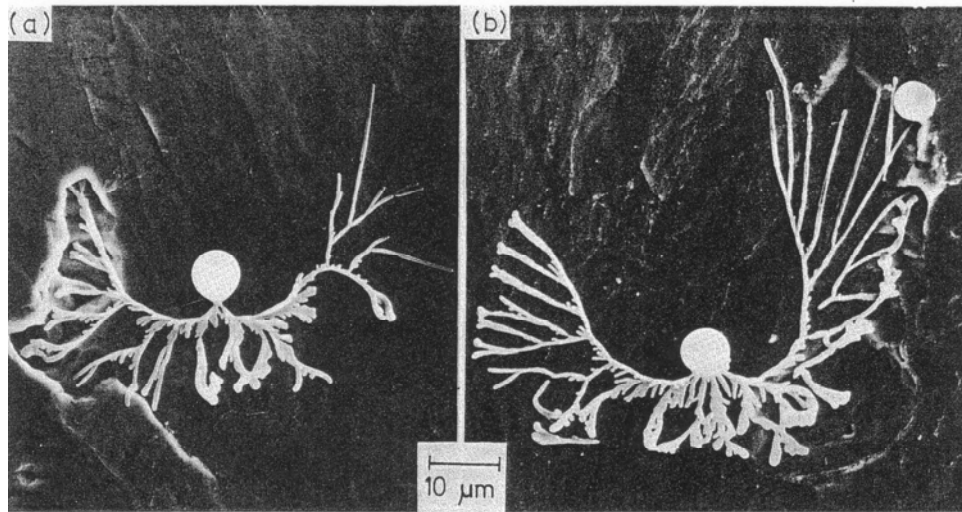
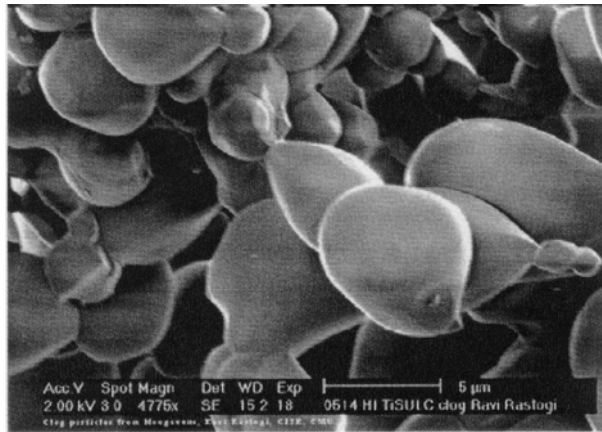
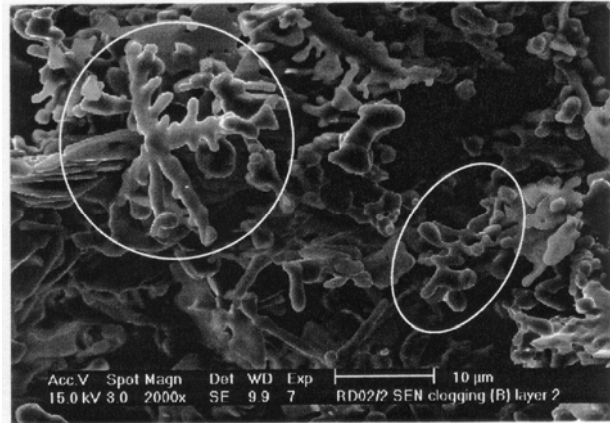


Fig. 36 Dendritic inclusions formed from a spherical primary silica in Fe-10%Ni alloy deoxidized with silicon (inclusions in ingot ^[189])



(a)



(b)

Fig.37 Alumina clogs at the submerged entry nozzle during continuous casting of low carbon Al-killed steel (a: Alumina inclusions clogged ^[39], b: Dendritic cluster and plate-like clusters clogs ^[40])

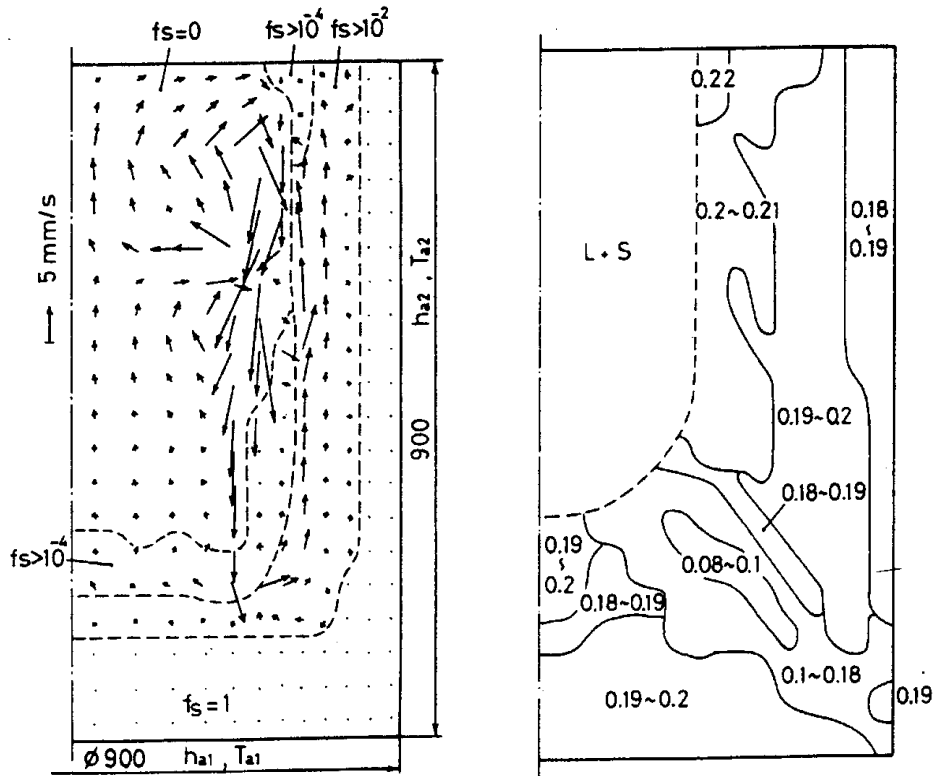


Fig. 38 Simulated fluid flow at 800s and macrosegregation at 3800s (numbers indicate carbon concentration in mass %) in a Fe-0.19%C ingot ^[218]

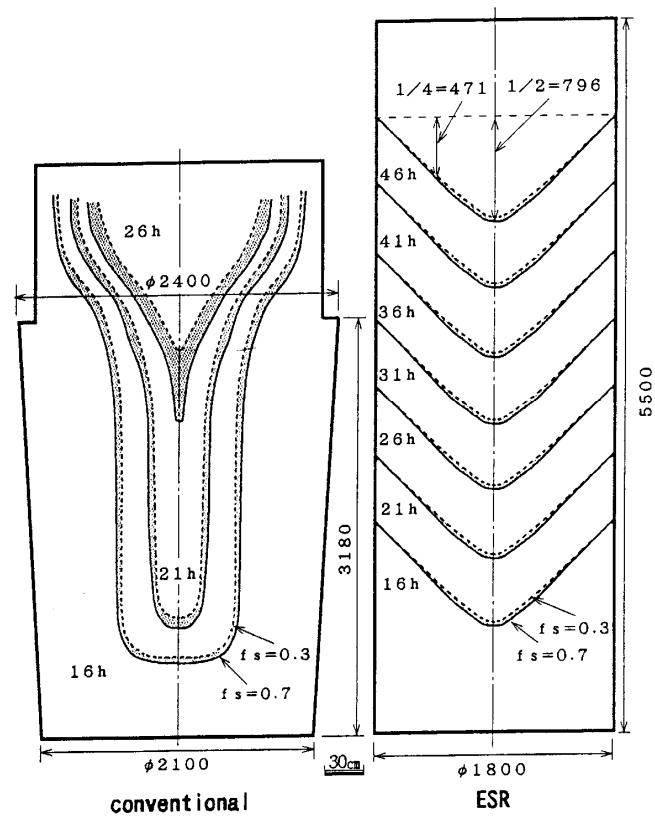


Fig. 39 Comparison of solidification pattern of a conventional melting furnace and ESR ^[230]

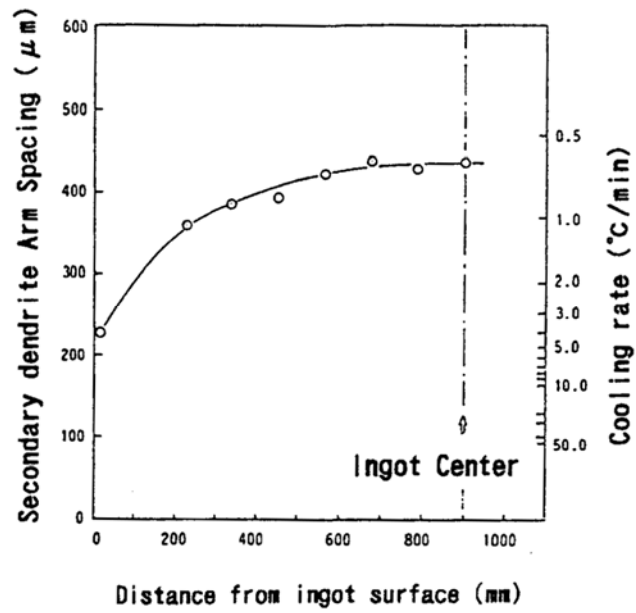


Fig. 40 Secondary dendrite arm spacing measured in 1800mm ϕ ESR ingot ^[230]

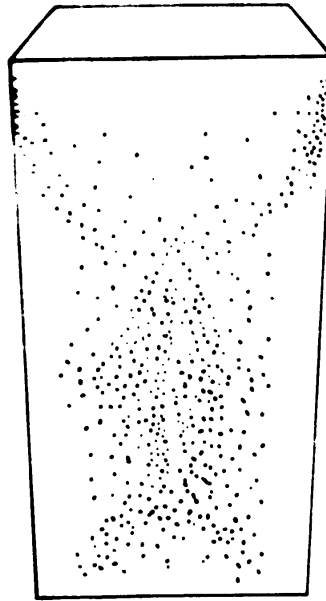


Fig. 41 Distribution of large slag inclusions in a top-poured 5 t ingot ^[14]

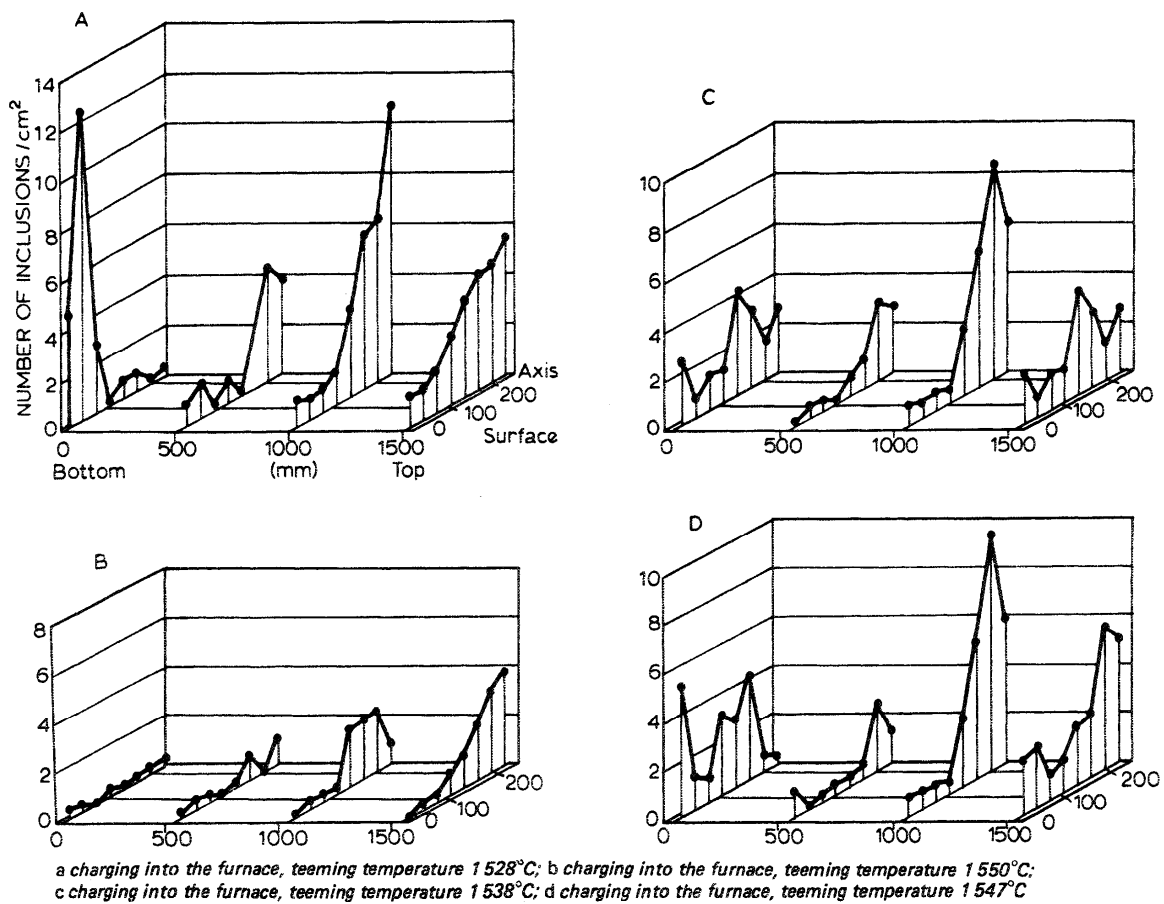


Fig. 42 Distribution of large inclusions in bottom-poured ingots at different teeming temperatures
[108]

References

1. J. Outten, "Reduce defects with direct pour technology," Foundry Management and Technology, Vol. 124 (8), 1996, 108-110.
2. P.F. Wieser, "Filtration of Irons and Steels," in Foundry Process-Their Chemistry and Physics, S. Katz and C.F. Landefeld, eds., Plenum Press, (New York-London), 1988, 495-512.
3. D. Apelian and K.K. Choi, "Metal Refining by Filtration," in Foundry Process-Their Chemistry and Physics, S. Katz and C.F. Landefeld, eds., Plenum Press, (New York-London), 1988, 467-494.
4. M. Blair, R.W. Monroe and J.A. Griffin, "A Review and Update of Advancements in Clean Cast Steel Technology," in Advances in the production and Use of Steel with Improved Internal Cleanliness, J.K. Mahaney, ed. American Society for Testing and Materials (ASTM), (West Conshohocken, USA), 1999, 57-72.
5. J.G. Bartholomew, R.L. Harvey and D.J. Hurtuk, "The Technology of Bottom Pour Fluxes," in 69th Steelmaking Conference Proceedings, ISS, Warrendale, PA, 1986, 121-127.
6. G. Auclair, M. Falcoz-Vigne, F. Lecouturier, J. Saleil, "Superclean Steel for Spring Applications," Wire Journal International, Vol. 31 (3), 1998, 84-89.
7. K. Sumitomo, M. Hashio, T. Kishida, A. Kawami, "Bottom Pouring and Ingot Quality at Sumitomo Metal Industries," Iron and Steel Engineer (3), 1985, 54-61.
8. , Steel Statistical Yearbook 2002, International Iron and Steel Institute, Brussels, 2002.
9. E. Fuchs and P. Jonsson, "Inclusion Characteristic in Bearing Steel Before and During Ingot Casting," High Temperature Materials and Processes, Vol. 19 (5), 2000, 333-343.
10. Schematic Illustration of Ingot Bottom Pouring Process. www.foseco-steel.com/pics/pic_products_ic_ov.gif.
11. T. Sjöqvist, M. Göransson, P. Jonsson, P. Cowx, "Influence of Ferromanganese Additions on Microalloyed Engineering Steel," Ironmaking and Steelmaking, Vol. 30 (1), 2003, 73-80.
12. P.K. Trojan, "Inclusion-forming reactions," ASM International, ASM Handbook, Vol. 15 (Casting), 1988, 88-97.
13. T.J. Baker and J.A. Charles, "Influence of Deformed Inclusions on the Short Transverse Ductility of Hot-rolled Steel," Effect of Second-Phase Particles on the Mechanical Properties of Steel, (Scarborough, UK), The Iron and Steel Institute, 1971, 88-94.
14. S.E. Lunner, "Origin and Types of Slag Inclusions in Non-Stabilized Austenitic Acid-Resistant Steel," in International Conference on Production and Application of Clean Steels, The Iron and Steel Institute, London, (Balatonfüred, Hungary), 1970, 124-136.

15. A.D. Wilson, "Clean Steel Technology-Fundamental to the Development of High Performance Steels," in Advances in the production and Use of Steel with Improved Internal Cleanliness, J.K. Mahaney, ed. American Society for Testing and Materials (ASTM), (West Conshohocken, USA), 1999, 73-88.
16. R. Kiessling, "Clean Steel- a debatable concept," Met. Sci., Vol. 15 (5), 1980, 161-172.
17. L. Zhang and B.G. Thomas, "State of the Art in Evaluation and Control of Steel Cleanliness," ISIJ Inter., Vol. 43 (3), 2003, 271-291.
18. J.A. Eckel, P.C. Glaws, J.O. Wolfe, B.J. Zorc, "Clean Engineering Steels-Process at the End of the Twentieth Century," in Advances in the production and Use of Steel with Improved Internal Cleanliness, J.K. Mahaney, ed. American Society for Testing and Materials (ASTM), (West Conshohocken, USA), 1999, 1-11.
19. T.B. Lund and L.K.P. Olund, "Improving Production, COntrol and Properties of Bearing Steels Intended for Demanding Applications," in Advances in the production and Use of Steel with Improved Internal Cleanliness, J.K. Mahaney, ed. American Society for Testing and Materials (ASTM), (West Conshohocken, USA), 1999, 32-48.
20. T. Uesugi, "Recent Development of Bearing Steel in Japan," Tetsu-to-Hagane, Vol. 74, 1988, 1889-1894.
21. D.C. Hilty and D.A.R. Kay, "Inclusions in Steel," Electric Furnace Steelmaking Conference Proceedings, Vol. 43, 1985, 237-251.
22. J.P. Bettembourg, J. Dieudonne, J.J. Gautier, F. Sauvage, "Study of Deoxidation by Aluminum on an Industrial Scale," in International Conference on Production and Application of Clean Steels, The Iron and Steel Institute, London, (Balatonfured, Hungary), 1970, 59-67.
23. E. Grethen and L. Philipe, "Kinetics of Deoxidation Reactions," in International Conference on Production and Application of Clean Steels, The Iron and Steel Institute, London, (Balatonfured, Hungary), 1970, 29-34.
24. J.A. Horwath and G.M. Goodrich, "Micro-inclusion Classification in Steel Casting," AFS Transactions, 1995, 495-510.
25. V.A. Kravchenko, V.M. Kirsanov, M.I. Staroseletskij, N.G. Miroshnichenko, A.G. Petrichenko, I.G. Uzlov, L.A. Moiseeva, "On variation of compositions of non-metallic inclusions in vacuum-processed steel wheel steel depending on its deoxidation method," Metallurgicheskaya i Gornorudnaya Promyshlennost' (Russia), Vol. 1 (1), 2000, 26-30.
26. K. Beskow, J. Jia, C.H.P. Lupis, D. Sichen, "Chemical Characteristics of Inclusions Formed at Various Stages during the Ladle Treatment of Steel," Ironmaking and Steelmaking, Vol. 29 (6), 2002, 427-435.

27. X. Zhang and M. Subramanian, "Thermodynamic Modeling for Deoxidation Control of Steel in LMF," 85th Steelmaking Conference Proceedings, ISS, Warrendale, PA, Vol. 85, 2002, 313-322.
28. K.R. Udupa, S. Subramanian, D.H. Sastry, G.N.K. Lyengar, "Studies on Inclusion Characterization in Electroslag Refined En24 Steel," Materials Forum, Vol. 17, 1993, 225-234.
29. T. Kawawa and M. Ohkubo, "A Kinetics on Deoxidation of Steel," Trans. ISIJ, Vol. 8, 1968, 203-219.
30. K. Asano and T. Nakano, "Deoxidation of Molten Steel with Deoxidizer," Trans. ISIJ, Vol. 12, 1972, 343-349.
31. E.T. Turkdogan, "Deoxidation of Steel," JISI, 1972, 21-36.
32. T. Fujisawa, "Deoxidation of Molten Steel and Physical Chemistry of Nonmetallic Inclusions," in Nishiyama Memorial Seminar, Vol. 126/127, ISS, Tokyo, 1988, 89-120.
33. K. Beskow, N.N. Viswanathan, L. Jonsson, D. Sichen, "Study of the Deoxidation of Steel with Aluminum Wire Injection in a Gas-Stirred Ladle," Metal. & Material Trans. B., Vol. 32B (2), 2001, 319-328.
34. D. Fan and G. Liu, "Discussion of Deoxidation Process in ASEA-SKF Ladle Refining Furnace," Steelmaking (in Chinese), Vol. 16 (1), 2000, 43-46.
35. H. Hosoda, N. Sano and Y. Matsushita, "Growth and Change of Deoxidation Products in Deoxidation with Silicon and Silicon-Manganese in Liquid Iron," Trans. ISIJ, Vol. 16, 1976, 115-121.
36. K. Nakanishi and J. Szekely, "Deoxidation Kinetics in a Turbulent Flow Field," Trans. ISIJ, Vol. 15, 1975, 522-530.
37. M. Olette and C. Gatellier, "Deoxidation of Liquid Steel," in Information Symposium of Casting and Solidification of Steel, Vol. 1, J.M. Gibb, ed. IPC Science and Technology Press Ltd, Guildford, 1977, 1-60.
38. R.A. Rege, E.S. Szekeres and W.D. Forgeng, "Three-Dimensional View of Alumina Clusters in Aluminum-Killed Low-Carbon Steel," Met. Trans. AIME, Vol. 1 (9), 1970, 2652.
39. R. Rastogi and A.W. Cramb, "Inclusion Formation and Agglomeration in Aluminum-killed Steels," in 2001 Steelmaking Conference Proceedings, Vol. 84, ISS, Warrendale, (Baltimore, Maryland, USA), 2001, 789-829.
40. R. Dekkers, B. Blanpain and P. Wollants, "Steel Cleanliness at Sidmar," in ISSTech2003 Conference Proceedings, ISS, Warrandale, PA, 2003, 197-209.
41. H. Ooi, T. Sekine and G. Kasai, "On the Mechanisms of Alunima Cluster Formation in Molten Iron," Trans. ISIJ, Vol. 15, 1975, 371-379.

42. C. Wagner, Zt. Elektrochemie, Vol. 65, 1961, 581-591.
43. W. Ostwald, Z. Phys. Chem., Vol. 34, 1900, 495.
44. M. Kahlweit, "Further Considerations on the Theory of Aging (Ostwald Ripening)," Berichte der Bunsen-Gesellschaft physikalische Chemie, Vol. 78 (10), 1974, 997-1001.
45. L. Ratke and W.K. Thieringer, "The Influence of Particle Motion on Ostwald Ripening in Liquids," Acta Metall., Vol. 33 (10), 1985, 1793-1802.
46. I.M. Lifshitz and V.V. Slyozov, J. Phys. Chem. Solids, Vol. 19 (35), 1961,
47. L. Zhang and B.G. Thomas, "Alumina Inclusion Behavior During Steel Deoxidation," 7th European Electric Steelmaking Conference, (Venice, Italy), Associazione Italiana di Metallurgia, Milano, Italy, Vol. II, 2002, 2.77-86.
48. L. Zhang, W. Pluschkell and B.G. Thomas, "Nucleation and Growth of Alumina Inclusions during Steel Deoxidation," in 85Steelmaking Conference Proceedings, Vol. 85, ISS, Warrandale, PA, 2002, 463-476.
49. R. Dekkers, B. Blanpain and P. Wollants, "Crystal Growth in Liquid Steel during Secondary Metallurgy," Metall. mater. trans., Vol. 34B, 2003, 161-171.
50. Z. Majewski, "Effect of Preliminary Deoxidation on the Precipitation of Non-Metallic Inclusions in Aging-Resistant Deep-Drawing Steels," in International Conference on Production and Application of Clean Steels, The Iron and Steel Institute, London, (Balatonfured, Hungary), 1970, 68-74.
51. F.B. Pickering, "Effect of Processing Parameters on the Origin of Non-Metallic Inclusions," in International Conference on Production and Application of Clean Steels, The Iron and Steel Institute, London, (Balatonfured, Hungary), 1970, 75-91.
52. Y. Miki, H. Kitaoka, T. Sakuraya, T. Fujii, "Mechanism for Separation of Inclusions from Molten Steel Stirred with a Rotating Electro-Magnetic Field," Tetsu-to-Hagane, Vol. 78 (3), 1992, 431-438.
53. I.N. Golikov, "Certain Peculiarities in the Formation of Oxide Inclusions Revealed by Complex Analysis," in International Conference on Production and Application of Clean Steels, The Iron and Steel Institute, London, (Balatonfured, Hungary), 1970, 35-41.
54. N. Aritomi and K. Gunji, "Inclusions in Iron Ingots Deoxidized with Aluminum and Solidified Unidirectionally," Trans. Jpn. Met., Vol. 22 (1), 1981, 43-56.
55. T. Sawai, M. Wakoh, Y. Ueshima, S. Mizoguchi, "Analysis of Oxide Dispersion During Solidification in Titanium, Zirconium-Deoxidized Steels," ISIJ Int., Vol. 32 (1), 1992, 169-173.

56. H. Goto, K.-I. Miyazawa, K.-I. Yamaguchi, S. Ogibayashi, K. Tanaka, "Effect of cooling rate on oxide precipitation during solidification of low carbon steels," ISIJ Int., Vol. 34 (5), 1994, 414-419.
57. Z. Ma and D. Janke, "Characteristics of oxide precipitation and growth during solidification of deoxidized steel," ISIJ Inter., Vol. 38 (1), 1998, 46-52.
58. Y.N. Malinochka, L.N. Nagnyuk and Y.S. Shmelev, "Globular Inclusions in Lightly Deoxidised Steels," Steel in the USSR, Vol. 20 (3), 1990, 136-138.
59. R. Dekkers, B. Blanpain and P. Wollants, "Steel Sampling to Study Inclusions," in ISSTech2003 Conference Proceedings, ISS, Warrandale, PA, 2003, 1007-1019.
60. S. Yang, "On Type and Distribution of Inclusions in F176 Steel," Iron & Steel (China), Vol. 22 (11), 1987, 11-16.
61. L. Zhang, B.G. Thomas and B. Rietow, "Investigation of Ingot Inclusions Using Microscope and SEM . Univ. of Illinois at Urbana-Champaign. IMF project report.," Report No. CCC200406, University of Illinois at Urbana-Champaign, 2004.
62. G. Pomey and B. Trentini, "Intriductory Address: Some Aspects of Cleanness in Steels," in International Conference on Production and Application of Clean Steels, The Iron and Steel Institute, London, (Balatonfured, Hungary), 1970, 1-14.
63. A.G. Franklin, "The Sampling Problem and the Importance of Inclusion Size Distribution," in International Conference on Production and Application of Clean Steels, The Iron and Steel Institute, London, (Balatonfured, Hungary), 1970, 241-247.
64. R. Jack, "Investigation and Metallographic Examination of Large Non-Metallic Inclusions in Fully Killed Steel," Met. Forum, Vol. 2 (2), 1979, 87-97.
65. T.B. Braun, J.F. Elliott and M.C. Flemings, "The Clustering of Alumina Inclusions," Metal. Trans. B, Vol. 10B (6), 1979, 171-184.
66. R. Rastogi and A.W. Cramb, "Inclusion Formation and Agglomeration in Aluminum-killed Steels", personal communication, 2003.
67. Special Report No.63, "Surface Defects in Ingots and Their Products," Report, Ingot Surface Defects Sub-Committee (Steelmaking Division) of the British Iron and Steel Research Association, 1958.
68. , Definitions and Causes of Continuous Casting Defects, The Iron and Steel Institute, London and Bradford, 1967.
69. V.B. Ginzburg and R. Ballas, "Chapter 15 Metallurgical Deffects in Cast Slabs and Hot Rolled Products," in Flat Rolling Fundamentals, Marcel Dekker, Inc., (New York . Basel), 2000, 354-378.

70. M. Byrne, T.W. Fenicle and A.W. Cramb, "The Sources of Exogenous Inclusions in Continuous Cast, Aluminum-Killed Steels," Steelmaking Conference Proceedings, Vol. 68, 1985, 451-461.
71. M. Byrne, T.W. Fenicle and A.W. Cramb, "The Sources of Exogenous Inclusions in Continuous Cast, Aluminum-Killed Steels," I & Smaker, Vol. 15 (6), 1988, 41-50.
72. M. Byrne, T.W. Fenicle and A.W. Cramb, "The Sources of Exogenous Inclusions in Continuous Cast, Aluminum-Killed Steels," ISS Trans., Vol. 10, 1989, 51-60.
73. H. Yin and H.T. Tsai, "Application of Cathodoluminescence Microscopy (CLM) in Steel Research," in ISSTech2003 Conference Proceedings, ISS, Warrandale, PA, 2003, 217-226.
74. R. Gass, H. Knoepke, J. Moscoe, R. Shah, J. Beck, J. Dzierzawski, P.E. Ponikvar, "Conversion of Ispat Inland's No.1 Slab Caster to Vertical Bending," in ISSTech2003 Conference Proceedings, ISS, Warrandale, PA, 2003, 3-18.
75. J.C.C. Leach, "Production of Clean Steel," in International Conference on Production and Application of Clean Steels, The Iron and Steel Institute, London, (Balatonfured, Hungary), 1970, 105-114.
76. M. Byrne and A.W. Cramb, "Operating Experience with Large Tundishes," I & Smaker, Vol. 15 (10), 1988, 45-53.
77. P. Rocabois, J.-N. Pontoire, V. Delville, I. Marolleau, "Different Slivers Type Observed in Solla Steel Plants and Improved Practice to Reduce Surface Defects on Cold Roll Sheet," in ISSTech2003 Conference Proceedings, ISS, Warrandale, PA, 2003, 995-1006.
78. Y.N. Malinochka, P.L. Litvinenko, V.S. Luchkin, V.A. Maslennikov, "Bright and Dark Bands on Rolled Sheets of 08Yu Steel," Steel in Translation, Vol. 22 (3), 1992, 144-147.
79. Y. Miki and S. Takeuchi, "Internal Defects of Continuous Casting Slabs Caused by Asymmetric Unbalanced Steel Flow in Mold," ISIJ Int., Vol. 43 (10), 2003, 1548-1555.
80. L. Zhang and S. Taniguchi, "Fundamentals of Inclusion Removal from Liquid Steel by Attachments to Rising Bubbles," I & Smaker, Vol. 28 (9), 2001, 55-79.
81. L. Zhang and S. Taniguchi, "Fundamentals of Inclusions Removal from Liquid Steel by Bubbles Flotation," International Materials Reviews, Vol. 45 (2), 2000, 59-82.
82. L. Zhang and S. Taniguchi, "Water Model Study on Inclusion Removal by Bubble Flotation from Liquid Steel by Bubble Flotation under Turbulent Condition," Ironmaking & Steelmaking, Vol. 29 (5), 2002, 326-336.
83. S. Dawson, N.D.G. Mountford, I.D. Sommerville, A. McLean, "The Evaluation of Metal Cleanliness in the Steel Industry Part I: Introduction," I & Smaker, Vol. 15 (7), 1988, 42-43.

84. S. Dawson, N.D.G. Mountford, I.D. Sommerville, A. McLean, "The Evaluation of Metal Cleanliness in the Steel Industry Part II," I & Smaker, Vol. 15 (8), 1988, 34-36.
85. S. Dawson, N.D.G. Mountford, I.D. Sommerville, A. McLean, "The Evaluation of Metal Cleanliness in the Steel Industry Part III," I & Smaker, Vol. 15 (9), 1988, 56-57.
86. S. Dawson, N.D.G. Mountford, I.D. Sommerville, A. McLean, "The Evaluation of Metal Cleanliness in the Steel Industry Part IV," I & Smaker, Vol. 15 (10), 1988, 54-55.
87. S. Dawson, N.D.G. Mountford, I.D. Sommerville, A. McLean, "The Evaluation of Metal Cleanliness in the Steel Industry Part V," I & Smaker, Vol. 15 (11), 1988, 63-64.
88. S. Dawson, N.D.G. Mountford, I.D. Sommerville, A. McLean, "The Evaluation of Metal Cleanliness in the Steel Industry Part VI," I & Smaker, Vol. 15 (12), 1988, 26-28.
89. S. Dawson, N.D.G. Mountford, I.D. Sommerville, A. McLean, "The Evaluation of Metal Cleanliness in the Steel Industry Part VII," I & Smaker, Vol. 16 (1), 1989, 44-45.
90. S. Dawson, N.D.G. Mountford, I.D. Sommerville, A. McLean, "The Evaluation of Metal Cleanliness in the Steel Industry Part VIII," I & Smaker, Vol. 16 (2), 1989, 36-37.
91. T.R. Allmand, "A Review of Methods for Assessing Nonmetallic Inclusions in Steel," JISI, Vol. 190, 1958, 359-372.
92. H. Suito, J. Takahashi and A. Karasev, "Issues on Inclusion Size Distribution Measurement," 11st Ultra-Clean Steel Symposium of High Temperature Process Committee of ISIJ, 1998, 1-20.
93. J. Angeli, H. Flobholzer, K. Jandl, T. Kaltenbrunner, W. Posch, H. Preblinger, "Qualitative and Quantitative Examinations of Microscopic Steel Cleanliness in Slab Samples," La Revue de Metallurgie - CIT, Vol. 96 (4), 1999, 521-527.
94. L. Zhang and K. Cai, "Project report: Cleanliness Investigation of Low Carbon Al-Killed Steel in Bao Steel," Report, BaoSteel, 1997.
95. T. Hansen and P. Jonsson, "Some ideas of Determining the Macro Inclusion Characteristic during Steelmaking," 2001 Electric Furnace Conference Proceedings, ISS, Warrendale, PA, Vol. 59, 2001, 71-81.
96. H. Matsuta, T. Sato and M. Oku, "Chemical Stete Analysis of Inclusions in IF Steel by EPMA and Auger Eletron Spectroscopy," ISIJ Int., Vol. 36 (Supplement), 1996, S125-127.
97. M. Goransson, F. Reinholdsson and K. Willman, "Evaluation of Liquid Steel Samples for the Determination of Microinclusion Characteristics by Spark-Induced Optical Emission Spectroscopy," I & Smaker, Vol. 26 (5), 1999, 53-58.
98. F. Ruby-Meyer and G. Willay, "Rapid Identification of Inclusions in Steel by OES-PDA Technique," Revue de Metallurgie-CIT, Vol. 94 (3), 1997, 367-378.

99. R. Meilland, H. Hocquaux, C. Louis, I. Pollino, F. Hoffert, "Rapid Characterization of Heterogeneities (Inclusions and Segregation) by Spectral Techniques," La Revue de Metallurgie - CIT, Vol. 96 (1), 1999, 88-97.
100. M. Burty, C. Louis, P. Dunand, P. Osmont, F. Ruby-Meyer, M. Nadif, F. Penet, T. Isono, E. Takeuchi, T. Toh, "Methodology of Steel Cleanliness Assessment," La Revue de Metallurgie - CIT, Vol. 97 (6), 2000, 775-782.
101. T. Saitoh, T. Kikuchi and K. Furuya, "Application of Laser Microprobe Mass Spectrometry (LAMMS) to a State Analysis of Non-metallic Inclusions and Precipitates in a Ti-added Ultra Low Carbon Steel," ISIJ Int., Vol. 36 (Supplement), 1996, S121-124.
102. N.K. Batia and H.H. Chaskelis, "Determination of Minimum Flaw Size Detectable by Ultrasonics in Titanium Alloy Plates," NDT International, Vol. 8, 1975, 261-264.
103. P. Bastien, "The Possibilities and Limitations of Ultrasonics in the Nondestructive Testing of Steel," NDT International, Vol. 10, 1977, 297-305.
104. B. Debiesme, I. Poissonnet, P. Choquet, F. Penet, "Steel Cleanliness at Sollac Dunkerque," Revue de Metallurgie-CIT, Vol. 90 (3), 1993, 387-394.
105. R. Eriksson, "Heat Transfer, Inclusion Characteristics and Fluid Flow Phenomena during Up-Hill Teeming," Thesis, Royal University of Technology, 2001.
106. P.C. Glaws, R.V. Fryan and D.M. Keener, "The Influence of Electromagnetic Stirring on Inclusion Distribution as Measured by Ultrasonic Inspection," in 74th Steelmaking Conference Proceedings, Vol. 74, ISS, Warrendale, PA, 1991, 247-264.
107. W. Betteridge and R.S. Sharpe, "The Study of Segregations and Inclusions in Steel by Microradiography," JISI, Vol. 158, 1948, 185-191.
108. M. Ichinoe, H. Mori, H. Kajioka, I. Kokubo, "Production of Clean Steel at Yawata Works," in International Conference on Production and Application of Clean Steels, The Iron and Steel Institute, London, (Balatonfured, Hungary), 1970, 137-166.
109. S.D. Strauss, "Nondestructive Examination," Power (June), 1983, s1-s16.
110. R.C. Sussman, M. Burns, X. Huang, B.G. Thomas, "Inclusion Particle Behavior in a Continuous Slab Casting Mold," in 10th Process Technology Conference Proc., Vol. 10, Iron and Steel Society, Warrendale, PA, (Toronto, Canada, April 5-8, 1992), 1992, 291-304.
111. T.E. Rooney and A.G. Stapleton, "The Iodine Method for the Determination of Oxides in Steel," JISI, Vol. 31, 1935, 249-254.
112. Y. Yoshida and Y. Funahashi, "Extraction and Size-Distribution Determination of Large Non-Metallic Inclusions in Steel by Slime Method," Trans. Iron Steel Inst. Jpn., Vol. 16 (11), 1976, 628-636.

113. Y. Nuri and K. Umezawa, "Development of Separation and Evaluation Technique of Non-metallic Inclusions in Steel by Electron Beam Melting," Tetsu-to-Hagane, Vol. 75 (10), 1989, 1897-1904.
114. Y. Murakami, "Inclusion Rating by Statistics of Extreme Values and Its Application on Fatigue Strength Prediction and Quality Control of Materials," Journal of Research of the National Institute of Standards and Technology, Vol. 99 (4), 1994, 345-351.
115. H. Kuguminato, Y. Izumiyama, T. Ono, T. Shiraishi, H. Abe, "Magnetic-Particle Testing for Micro-Inclusion Detection on Tinplate for Drawn and Ironed (DI) Can," Kawasaki Steel Tech. Rep., Vol. 12 (2), 1980, 331-338.
116. G.R. Webster, J.M. Madritch, G.A. Perfetti, L.C. Wong, "Inclusion Detection in Tin Mill Products Using Magnetic Particle Method," Iron & Steelmaker, Vol. 12 (10), 1985, 18-27.
117. A.S. Venkatadri, "Mechanism of Formation of Non-metallic Inclusions in Aluminum-killed Steel," Trans. ISIJ, Vol. 18, 1978, 591-600.
118. A. Chino, Y. Kawai, H. Kutsumi, M. Kawakami, "Applicability of Several Estimation Methods of Inclusions in Steel," ISIJ Int., Vol. 36 (Supplement), 1996, S144-147.
119. T.L. Mansfield, "Ultrasonic Technology for Measuring Molten Aluminum Quality," Mater. Eval., Vol. 41 (6), 1983, 743-747.
120. S. Dawson, D. Walker, N. Mountford, I.D. Sommerville, A. McLean, "The Application of Ultrasonics to Steel Ladle Metallurgy," Canadian Institute of Mining and Metallurgy, 1988, 80-91.
121. R.I.L. Guthrie and H.C. Lee, "On-Line Measurements of Inclusions in Steelmaking Operations," Steelmaking Conference Proceedings, (Toronto), ISS, Warrendale, PN15086, USA, Vol. 75, 1992, 799-805.
122. R.I.L. Guthrie, "On the Detection, Behavior and Control of Inclusions in Liquid Metals," in Foundry Process-Their Chemistry and Physics, S. Katz and C.F. Landefeld, eds., Plenum Press, (New York-London), 1988, 447-466.
123. H. Yin, H. Shibata, T. Emi, M. Suzuki, "'In-situ' Observation of Collision, Agglomeration and Cluster Formation of Alumina Inclusions Particles on Steel Melts," ISIJ Int., Vol. 37 (10), 1997, 936-945.
124. H. Yin, H. Shibata, T. Emi, M. Suzuki, "Characteristics of Agglomeration of Various Inclusion Particles on Molten Steel Surface," ISIJ Int., Vol. 37 (10), 1997, 946-955.
125. H. Shibata, H. Yin, S. Yoshinaga, T. Emi, M. Suzuki, "'In-situ' Observation of Engulfment and Pushing of Nonmetallic Inclusions in Steel Melt by Advancing Melt/Solid Interface," ISIJ Int., Vol. 38 (2), 1998, 149-156.
126. S. Makarov, R. Ludwig and D. Apelian, "Electromagnetic Visualization Technique for Non-metallic Inclusions in a Melt," Meas. Sci. Technol., Vol. 10 (11), 1999, 1047-1053.

127. J. Schade, "The Measurement of Steel Cleanliness," Steel Technology International, 1993, 149.
128. M.T. Burns, J. Schade and C. Newkirk, "Recent Developments in Measuring Steel Cleanliness at Armco Steel Company," in 74th Steelmaking Conference Proceedings, Vol. 74, ISS, Warrendale, PA, 1991, 513-523.
129. C. Bonilla, "Slivers in Continuous Casting," in 78th Steelmaking Conference Proceedings, Vol. 78, ISS, Warrendale, PA, 1995, 743-752.
130. K. Ito, "Science of Molten Steel Production," 165th-166th Nishiyama Memorial Seminar, (ISIJ, Tokyo), 1997, 1-24.
131. M. Olette and C. Catellier, "Effect of additions of calcium, magnesium or rare earth elements on the cleanness of steels.," 2nd Int. Conf. on Clean Steel, (Balatonfured, Hungary), Metal Soc., London, UK, 1983, 165-185.
132. S. Armstrong, "Tundish Practices at Weirton Steel for Improved Steel Cleanliness," in 76th Steelmaking Conference Proceeding, Vol. 76, ISS, Warrendale, PA, 1993, 475-481.
133. S.D. Melville and L. Brinkmeyer, "Evaluating Steelmaking and Casting Prectice Which Affect Quality," in 78th Steelmaking Conference Proceedings, ISS, Warrendale, PA, 1995, 563-569.
134. R.L. Shultz, "Attack of Alumino-Silicate Refractories by High Manganese Steel," Steelmaking Conference Proceedings, Vol. 62, 1979, 232-235.
135. A. Yamanaka and H. Ichiashi, "Dissolution of Refractory Elements to Titanium Alloy in VAR," ISIJ Inter., Vol. 32 (5), 1992, 600-606.
136. R. Tsujino, A. Tanaka, A. Imamura, D. Takahashi, S. Mizoguchi, "Mechanism of Deposition of Inclusions and Metal on ZrO₂-CaO-C Immersion Nozzle in Continuous Casting," Tetsu-to-Hagane, Vol. 80 (10), 1994, 31-36.
137. G.B. Hassall, KG; Jones, N; Warman, M, "Modelling of Ladle Glaze Interactions," Vol. 29 (5), 2002, 383-389.
138. M.D. Maheshwari, T. Mukherjee and J.J. Irani, "Inclusion Distribution in Ingots as Guide to Segregation Mechanism," Ironmaking and Steelmaking, Vol. 9 (4), 1982, 168-177.
139. S. Riaz, K.C. Mills and K. Bain, "Experimental Examination of Slag/Refractory Interface," Ironmaking and Steelmaking, Vol. 29 (2), 2002, 107-113.
140. J.M. Middleton and B. Cauwood, "Exogenous Inclusions in Steel Castings," Brit. Foundryman, Vol. 60 (8), 1967, 320-330.
141. G. Benko, S. Simon and G. Szarka, "Tracing the Origin of Exogenous Oxide Inclusions in Killed and Rimming Steels by Mean of Subsequesntly Activated Tracer Elements," Neue Hutte, Vol. 17 (1), 1972, 40-44.

142. H. Zeder and L. Pocze, "Marking of Refractory Materials With Inactive Tracers to Determine the Origins of Exogenous Inclusions in Steel," Berg Huttenmann. Monatsh., Vol. 125 (1), 1980, 1-5.
143. T. Komai, "Source of Exogenous Inclusions and Reduction of Their Amount in the Continuous Casting Process," Tetsu-to-Hagane, Vol. 67 (8), 1981, 1152-1161.
144. M. Burty, P. Dunand, J. Ritt, H. Soulard, A. Blanchard, G. Jeanne, F. Penet, R. Pluquet, I. Poissonnet, "Control of DWI Steel Cleanliness by Lanthanum Tracing of Deoxidation Inclusions Ladle Slag Treatment and a Methodical Approach," Ironmaking Conference Proceedings, Vol. 56, 1997, 711-717.
145. L. Zhang and K. Cai, "Project Report: Cleanliness Investigation of Low Carbo Al-Killed Steel Produced by LD-RH-CC Process at WISCO," Report, 1995.
146. X. Zhang and K. Cai, "Project Report: Investigation of Inclusion Behavior of 16MnR Steel at WISCO," Report, 1996.
147. Y. Furuya, S. Matsuoka and T. Abe, "Inclusion Inspection Method in Ultra-sonic Fatigue Test," Tetsu-to-Hagane, Vol. 88 (10), 2002, 643-650.
148. J.D. Thomas, R.O. Russell and T.R. Garcia, "The Entrapment of Gross Nonmetallics during Early pulls of the Ingots from the Teeming Platform," in 69th Steelmaking Conference Proceedings, ISS, Warrendale, PA, 1986, 300-308.
149. A.W. Cramb. Inclusion Formation during Foundry Processing, <http://neon.mems.cmu.edu/afs/afs2/window2.html>. (1996),
150. R. Topno, D.S. Gupta, U.P. Singh, B. Roy, S. Jha, "Improvement in the surface quality of ball bearing steel rounds at Bar Mill," Scandinavian Journal of Metallurgy, Vol. 31 (1), 2002, 20-24.
151. J.M. Svoboda, R.W. Monroe, C.E. Bates, J. Griffin, "Appearance and Composition of Macro-inclusions in Steel Castings," AFS Transactions, 1987, 187-202.
152. R. Schlatter, "Review of Teeming Stream Protection Systems for Ingot Casting," Steel Times (8), 1986, 432-436.
153. T.J. Ward, R.F. Schmehl and F.A. Vonesh, "A New Technique for Inert Gas Shrouding of Molten Metal Streams," in 67th Steelmaking Conference Proc, Vol. 67, ISS, Warrendale, PA, 1984, 97-102.
154. T.W. Scamman and S.J. Miller, "The Effect of Argon Shrouding of Stainless Ingots on Inclusion Lines," in 67th Steelmaking Conference Proc, Vol. 67, ISS, Warrendale, PA, 1984, 39-44.
155. R.D. O'Hara, A.G.R. Spence and J.D. Eisenwasser, "Protection of the Pouring Stream and Mould Purging with Carbon Dioxide," Revue de Metallurgie-CIT, Vol. 84 (2), 1987, 147-234.

156. N.A. Zyuban and S.I. Zhul'ev, "Features of the Formation of Endogenic Inoculants in the Metal Stream during the Casting of Large Ingots," Metallurgist, Vol. 44 (9-10), 2000, 530-533.
157. A. Staronka and W. Golas, "Wettability of Solid CaO-MgO-SiO₂ and Al₂O₃-SiO₂-CaO Oxides by Liquid Steel," Arch. Eisenhüttenwes., Vol. 51 (10), 1980, 403-406.
158. P. Kazakevitch and M. Olette, "Role of Surface Phenomena in the Mechanism of Removal of Solid Inclusions," in International Conference on Production and Application of Clean Steels, The Iron and Steel Institute, London, (Balatonfüred, Hungary), 1970, 42-49.
159. A.W. Cramb and I. Jimbo, "Interfacial Considerations in Continuous Casting," Iron & Steelmaker (ISS Trans.), Vol. 11, 1990, 67-79.
160. M.D. Maheshwari and T. Mukherjee, "Inclusions in a 0.5%C Bottom Poured Killed Steel Ingot," Tisco, Vol. 26 (1), 1979, 9-18.
161. H. Nagayama, "Mineral Study of the Source of Exogenous Inclusions in Steel," Tetsu-to-Hagane, Vol. 56 (13), 1970, 1699-1715.
162. R. Datta, A. Prasad, S. Kumar, V. Bhusan, N.S. Mishra, "Genesis of Exogenous Inclusions in Concast Plate Products," Steel Times International, Vol. 15 (2), 1991, 40-41.
163. L. Zhang, B.G. Thomas, K. Cai, L. Zhu, J. Cui, "Inclusion Investigation during Clean Steel Production at Baosteel," in ISSTech2003, ISS, Warrendale, PA, 2003, 141-156.
164. K. Suzuki, K. Taniguchi and T. Takenouchi, "Study of Behavior of Exogenous Inclusions in Large Forging Ingots. Pt. 1-2," Tetsu-to-Hagane, Vol. 61 (4), 1975, S96-97.
165. T. Wei and F. Oeters, "A Model Test for Emulsion in Gas-Stirred Ladles," Steel Research, Vol. 63 (2), 1992, 60-68.
166. M. Iguchi, Y. Sumida, R. Okada, Z. Morita, "Evaluation of the Critical Gas Flow Rate Using Water Model for the Entrapment of Slag Into a Metal Bath Subject to Gas Injection," Tetsu-to-Hagane, Vol. 79 (5), 1993, 569-575.
167. S.-H. Kim and R.J. Fruehan, "Physical Modeling of Liquid/Liquid Mass Transfer in Gas Stirred Ladles," Metall. Trans. B, Vol. 18B (2), 1987, 381-390.
168. R. Sankaranarayanan and R.I.L. Guthrie, "A Laboratory Study of Slag Entrainment during the Emptying of Metallurgical Vessels," Steelmaking Conference Proceedings, (Toronto), ISS, Warrendale, PN15086, USA, Vol. 75, 1992, 655-664.
169. I. Manabu, S. Yutaka, O. Ryusuke, M. Zen-Ichiro, "Evaluation of the Critical Gas Flow Rate Using Water Model for the Entrapment of Slag into a Metal Bath Subject to Gas Injection," Tetsu-to-Hagane, Vol. 79 (5), 1993, 33.
170. H.F. Marston, "High Quality Ingots: The Design of Bottom Pouring Powders," in 69th Steelmaking Conference Proceedings, ISS, Warrendale, PA, 1986, 107-119.

171. I.N. Zigalo, "Experimental Investigation of Metal Hydrodynamics During Bottom Pouring," Steel in the USSR, Vol. 19 (7), 1989, 281-284.
172. R. Eriksson, L. Jonsson and P.G. Jonsson, "Effect of Entrance Nozzle Design on the Fluid Flow in an Ingot Mold during Filling," ISIJ International, Vol. 44 (8), 2004, 1358-1365.
173. L. Zhang and B.G. Thomas, "Fluid flow and inclusion motion during ingot teeming process-Part I: fluid flow," Report, Continuous Casting Consortium, University of Illinois at Urbana-Champaign, 2005.
174. A.P. Ogurtsov, "Dependence of Optimum Bottom Pouring Rate on Steel Level in Mould," Steel in the USSR, Vol. 18, 1988, 225-227.
175. L. Zhang and B.G. Thomas, "Fluid flow and inclusion motion during ingot teeming process-Part II: free surface phenomena," Report, Continuous Casting Consortium, University of Illinois at Urbana-Champaign, 2005.
176. A. Halvae and J. Campbell, "Critical Mold Entry Velocity for Aluminum Bronze Castings," AFS Transactions, 1998, 35-46.
177. J.M. Harman and A.W. Cramb, "A Study of the Effect of Fluid Physical Properties upon Droplet Emulsification," in Steelmaking Conference Proceedings, Vol. 79, ISS, Warrendale, PA, 1996, 773-784.
178. Y.N. Malinochka, A.N. Kurasov, E.P. Ionts, V.A. Tishkov, T.I. Makogonova, "Nature of Coarse Inclusions in Ingots of Low Alloy Steels," Steel in the USSR, Vol. 20 (1), 1990, 50-54.
179. M.M. McDonald and D.C. Ludwigson, "Fractographic Examination in the Scanning Electron Microscope as a Tool in Evaluating Through-Thickness Tension Test Results," ASTM J. Test. Eval., Vol. 11 (3), 1983, 165-173.
180. P.W. Wright, "The Origins of Exogenous Inclusions: Some Observations," Met. Forum, Vol. 2 (2), 1979, 82-86.
181. N.N. Tripathi, M. Nzotta, A. Sandberg, S. Du, "Effect of Ladle Age on Formation of Non-Metallic Inclusions in Ladle Treatment," Ironmaking & Steelmaking, Vol. 31 (3), 2004, 235-240.
182. N.N. Tripathi, M. Nzotta, A. Sandberg, S. Du, "Identification of Inclusions Generated by Slag-Refractory Reactions," Steel Grips, Vol. 2 (1), 2004, 40-47.
183. S. Du, A. Sandberg and N. Tripathi, "A Study on the Population and Chemical Characterization of Non-Metallic Inclusions in the Tool Steel Making Process," in ICS 2005 - The 3rd International Congress on the Science and Technology of Steelmaking, AIST, Warrendale, PA, (May 9-12, 2005, Charlotte, NC), 2005, 649-660.
184. L. Ferro, J. Petroni, D. Dalmaso, J. Madias, C. Cicutti, "Steel Cleanliness in Continuous Casting Slabs," Steelmaking Conference Proceeding, (Warrendale, PA), ISS, Vol. 79, 1996, 497-502.

185. T. Sjoqvist, S. Jung, P. Jonsson, M. Andreasson, "Influence of Calcium Carbide Slag Additions on Inclusions Characteristics in Steel," Ironmaking and Steelmaking, Vol. 27 (5), 2000, 373-380.
186. K. Larsen and R.J. Fruehan, "Calcium Modification of Oxide Inclusions," Iron & Steelmaker (ISS Trans.), Vol. 12, 1991, 125-132.
187. K. Takachio and T. Nonomura, "Improvement in the quality of superalloy VAR ingots," ISIJ Inter., Vol. 36 (Supplement), 1996, Suppl., S85-S88.
188. Y. Miki, H. Kitaoka, T. Sakuraya, T. Fujii, "Mechanism for Separating Inclusions from Molten Steel Stirred with a Rotating Electro-Magnetic Field," ISIJ Inter., Vol. 32 (1), 1992, 142-149.
189. N. Aritomi and K. Gunji, "On the Formation of Dendritic Inclusion from a Spherical Primary Silica in Iron-10% Nickel Alloy Deoxidized with Silicon," Trans. ISIJ, Vol. 20, 1980, 26-32.
190. H. Tozawa, Y. Kato, K. Sorimachi, T. Nakanishi, "Agglomeration and Flotation of Alumina Clusters in Molten Steel," ISIJ Inter., Vol. 39 (5), 1999, 426-434.
191. Y. Miki and B.G. Thomas, "Modeling of Inclusion Removal in a Tundish," Metall. Mater. Trans. B, Vol. 30B (4), 1999, 639-654.
192. R.B. Snow and J.A. Shea, J. Am. Ceram. Soc., Vol. 32 (6), 1949, 187-194.
193. G.C. Duderstadt, R.K. Iyengar and J.M. Matesa, AIME Proc. Electric Furnace Conference, 1967, 61-66.
194. J.W. Farrell and D.C. Hilty, AIME Proc. Electric Furnace Conference, 1971, 31-46.
195. K. Schwerdtfeger and H. Schrewe, AIME Proc. Electric Furnace Conference, 1970, 95-104.
196. E. Steinmetz, H. Lindborg, W. Morsdorf, D. Hammerschmid, Arch. Eisenhutten, Vol. 48 (11), 1977, 569-574.
197. S.K. Saxena, H. Sandberg, T. Waldenstrom, A. Persson, S. Steensen, "Mechanism of Clogging of Tundish Nozzle during Continuous Casting of Aluminium-killed Steel," Scandinavian Journal of Metallurgy, Vol. 7, 1978, 126-133.
198. S. Dawson, "Tundish Nozzle Blockage During the Continuous Casting of Aluminum-killed Steel," in 73rd Steelmaking Conference Proc., Vol. 73, ISS, Warrendale, PA, 1990, 15-31.
199. Y. Fukuda, Y. Ueshima and S. Mizoguchi, "Mechanism of Alumina Deposition on Alumina Graphite Immersion Nozzle in Continuous Caster," ISIJ International, Vol. 32, 1992, 164-168.
200. W. Tiekink and A. Pieters, in 77th Steelmaking Conference Proceeding, Vol. 77, ISS, Warrendale, PA, 1994, 423-427.

201. Ichikawa, Taikabutsu Overseas, Vol. 14 (2), 1994, 52-53.
202. F. Fuhr, C. Cicutti, G. Walter, G. Torga, "Relationship Between Nozzle Deposits and Inclusion Composition in the Continuous Casting of Steel," in ISSTech2003 Conference Proceedings, ISS, Warrendale, PA, 2003, 165-175.
203. F.L. Kemeny, "Tundish Nozzle Clogging - Measurement and Prevention," in McLean Symposium Proceedings, ISS, Warrendale, PA, 1998, 103-110.
204. B.G. Thomas and H. Bai, "Tundish Nozzle Clogging ?Application of Computational Models," 78th Steelmaking Conf. Proc., Iron and Steel Society, Warrendale, PA, 2001, 895-912.
205. M.C. Schneider and C. Beckermann, "The Formation of Macrosegregation by Multicomponent Thermosolutal Convection during the Solidification of Steel," Metall. Mater. Trans. A, Vol. 26A (9), 1995, 2373-2388.
206. B.G. Thomas, "Modelling and Simulation for Casting and Solidification: Theory and Application," in "Continuous Casting of Steel, Chap.15," O. Yu, ed. Marcel Dekker, New York, 2000.
207. B.G. Thomas, R. O'Malley, T. Shi, Y. Meng, D. Creech, D. Stone, "Validation of Fluid Flow and Solidification Simulation of a Continuous Thin Slab Caster," in Modeling of Casting, Welding, and Advanced Solidification Processes, Vol. IX, Shaker Verlag GmbH, Aachen, Germany, (Aachen, Germany, August 20-25, 2000), 2000, 769-776.
208. J. Parkman, "Simulation of Thermal-Mechanical Behavior During Initial Solidification of Steel," M.S. Thesis, University of Illinois, 2000.
209. L. Zhang, "Mathematical Simulation of Fluid Flow in Gas-Stirred Liquid Systems," Modelling Simul. Mater. Sci. Eng., Vol. 8 (4), 2000, 463-476.
210. L. Zhang and S. Taniguchi, "Fluid Flow and Inclusion Removal in Continuous Casting Tundish," Metal. & Material Trans. B., Vol. 31B (2), 2000, 253-266.
211. B.G. Thomas and L. Zhang, "Mathematical Modeling of Fluid Flow in Continuous Casting," ISIJ Inter., Vol. 41 (10), 2001, 1181-1193.
212. Z.A. Xu and F. Mampaey, "Experimental and Simulation Study on Mold Filling With Various Gating Systems," AFS Transactions, 1996, 155-166.
213. C.W. Hirt and B.D. Nichols, "Volume of Fluid (VOF) Method for the Dynamics of Free Boundary," J. Comput. Phys., Vol. 39 (1), 1981, 201-225.
214. Z.A. Xu and F. Mampaey, "Experimental and Simulation Study on Mold filling Coupled with Heat Transfer," AFS Transactions, 1994, 181-190.

215. J. Delorme, M. Laubin and H. Maas, "Solidification of Large Forging Ingots," in Information Symposium of Casting and Solidification of Steel, Vol. 1, J.M. Gibb, ed. IPC Science and Technology Press Ltd, Guildford, 1977, 214-277.
216. Y. Tsuchida, M. Nakada, Y. Kunisada, T. Teshima, "Influence of Ingot Shape and Chemical Composition on the Inverse-V Segregation in Killed Steel Ingots," Tetsu-to-Hagane, Vol. 73 (9), 1987, 1125-1132.
217. J.J. Moore and N.A. Shah, "Mechanisms of Formation of A- and V-segregation in Cast Steel," Internaitonal Metals Reviews, Vol. 28 (6), 1983, 338-356.
218. I. Ohnaka and M. Matsumoto, "Computer Simulation of Macrosegregation in Ingots," Tetsu-to-Hagane, Vol. 73 (14), 1987, 1698-1705.
219. H. Yamada, T. Sakurai, T. Takenouchi, Y. Iwanami, "Estimation of Forming Condition of Center Porosity in Forging Ingot," Tetsu-to-Hagane, Vol. 73 (14), 1987, 1706-1713.
220. R.D. Pehlke, "Formation of Porosity Solidification of Cast Metals," in Foundry Process-Their Chemistry and Physics, S. Katz and C.F. Landefeld, eds., Plenum Press, (New York-London), 1988, 427-446.
221. C. Beckermann, "Modeling of Macrosegregation: Past, Present and Future," in Fleming Symposium, TMS, Warrendale, PA, (Boston, MA, June 2000), 2000.
222. C.Y. Wang and C. Beckermann, "A Multiphase Solute Diffusion Model for Dendritic Alloy Solidification," Metall. Mater. Trans., Vol. 24A, 1993, 2787-2802.
223. B.G. Thomas, I.V. Samarasekera and J.K. Brimacombe, "Mathematical Model of the Thermal Processing of Steel Ingots, Part II: Stress Model," Metall. Trans. B, Vol. 18B (1), 1987, 131-147.
224. B.G. Thomas, I.V. Samarasekera and J.K. Brimacombe, "Application of Mathematical Heat Flow and Stress Models of Steel Ingot Casting to Investigate Panel Crack Formation," in Modeling of Casting and Welding Processes III, Vol. 3, S. Kou and R. Mehrabian, eds., TMS, Warrendale, PA, (Santa Barbara, CA), 1987, 479-495.
225. B.G. Thomas, I.V. Samarasekera and J.K. Brimacombe, "Mathematical Model of the Thermal Processing of Steel Ingots, Part I: Heat Flow Model," Metall. Trans., Vol. 18B (1), 1987, 119-130.
226. M.C. Flemings, "Our understanding of macrosegregation: past and present," ISIJ International, Vol. 40 (9), 2000, 833-841.
227. D. Deng, "Accumulation of Inclusions and Segregation in RE Treated Steel," Iron & Steel (China), Vol. 21 (8), 1986, 37-43.

228. S.I. Zhul'ev and N.A. Zyuban, "Effect of Process Parameters in the Casting of Large Forging Ingots on the Formation of the Optimum Structure in the Axial Zone," Metallurgist, Vol. 45 (11-12), 2001, 484-489.
229. V.A. Tyurin, V.V. Romanenko and V.P. Romanenko, "Study of the macrostructure of long forging ingots," Metallurgist, Vol. 45 (9-10), 2001, 419-422.
230. I.S. Asano, T; Funasaki, M; Takenouchi, T; Yamata, H, "Construction and operation of a new melting shop at Muroran Plant of JSW," Tetsu-to-Hagane, Vol. 81 (5), 1995, T16-T18.
231. K. Mukai and W. Lin, "Behavior of Non-metallic Inclusions and Bubbles in Front of Solidifying Interface of Liquid Iron," Tetsu-to-Hagane, Vol. 80 (7), 1994, 533-538.
232. K. Mukai and W. Lin, "Motion of Small Particles in Solution with a Interfacial Tension Gradient and Engulfment of the Particles by Solidifying Interface," Tetsu-to-Hagane, Vol. 80 (7), 1994, 527-532.
233. K. Mukai, "Engulfment and Pushing of Foreign Particles Such As Inclusions and Bubbles at Solidifying Interface," Tetsu-to-Hagane, Vol. 82 (1), 1996, 9-14.
234. G. Wilde and J.H. Perepezko, "Experimental study of particle incorporation during dendritic solidification," Materials Science and Engineering A (Switzerland), Vol. 283 (1-2), 2000, 25-37.
235. Q. Yuan and B.G. Thomas, "Transport and Entrapment of Particles in Continuous Casting of Steel," in ICS 2005 - The 3rd International Congress on the Science and Technology of Steelmaking, AIST, Warrendale, PA, (May 9-12, 2005, Charlotte, NC), 2005, 745-759.
236. Q. Yuan, B.G. Thomas and S.P. Vanka, "Study of Transient Flow and Particle Transport during Continuous Casting of Steel Slabs, Part 2. Particle Transport.," Metal. & Material Trans. B, Vol. 35B (4), 2004, 703-714.
237. Z. Chen, J. Liu and J. Zeng, "Study on the Effect of Rare Earth on the Inclusion Morphology of Spring Steel 60Si2Mn," Iron & Steel (China), Vol. 18 (3), 1983, 43-49.
238. X. Zhu, W. Liu, Y. Ding, J. Su, J. Zhou, M. Jiang, X. Wu, "Numerical Simulation on the Formation of Bottom Cone of Inclusions in Large Steel Ingots," Xi'an Jiaotong Daxue Xuebao (Journal of Xi'an Jiaotong University), Vol. 24 (5), 1990, 71-78.
239. Q. Xu, F. Lou and D. Luo, "Analysis of the Formation of Large Inclusions at the Bottom of Uphill-Teemed Rail Steel Ingot," Iron & Steel (China), Vol. 22 (1), 1987, 9-15.
240. Y. Wei, L. Dong, X. Liu, Z. Yang, R. Sun, "Effects of Exothermic Powder on Large-Sized Inclusions in the Cone Above the Ingot Bottom," Iron & Steel (China), Vol. 21 (9), 1986, 18-22.
241. L. Dong, X. Liu and Y. Wei, "Research on the Mechanism for the Accumulation of Large Oxide Inclusions at the Bottom of Ingots," J. Beijing Univ. Iron Steel Technol., (1), 1986, 23-32.

242. Z. Liu and K. Cai, "Purity Steel Production Technology," Iron & Steel (in Chinese), Vol. 35 (2), 2000, 64-69.
243. A.W. Cramb, "High Purity, Low Residual and Clean Steels," in Impurities in Engineered Materials: Impact, Reliability and Control, C.L. Briant, ed. Marcel Dekker Inc., (New York), 1999, 49-89.
244. K. Ogawa, "Slag Refining for Production of Clean Steel," in Nishiyama Memorial Seminar, Vol. 143/144, Iron and Steel Institute of Japan, (ISS, Tokyo), 1992, 137-166.
245. H. Gao, "Source and Control Measures of Hydrogen, Nitrogen and Oxygen in Steel," Steelmaking (in Chinese), Vol. 16 (2), 2000, 38-43.
246. H. Lachmund, B. Prothmann, D. Huin, H.S. Raymond, H. Gaye, "Nitrogen Alloying of Liquid Steel by Gas Injection in the Ladle and/or Converter," La Revue de Metallurgie - CIT, Vol. 95 (4), 1998, 487-499.
247. Mori, Tetsu-to-Hagane, Vol. 51, 1965, 1930.
248. G.B.V.D. Graaf, H.E.A.V.D. Akker and L. L. Katgerman, "A Computational and Experimental Study on Mold Filling," Metal. & Material Trans. B., Vol. 32B (1), 2001, 69-78.
249. C.P. Hong, S.Y. Lee and K. Song, "Development of a new simulation method of mold filling based on a body-fitted coordinate system," ISIJ Inter., Vol. 41 (9), 2001, 999-1005.
250. H.J. Lin, "Modeling of Fluid Flow and Partial Solidification during Mold filling," AFS Transactions, 1999, 777-782.
251. H.Y. Yuan, H.T. Lin and G.X. Sun, "Simulation and Experimental Study on Postfilling Flow and Its Influence on Solidification," AFS Transactions, 1997, 723-932.
252. X. Xue, S.F. Hansen and P.N. Hansen, "Numerical Simulation and Experimental Verification of Mold Filling Processes Through Depressurized and Less-Depressurized Gating Systems," AFS Transactions, 1993, 549-558.
253. X. Xue, S.F. Hansen and P.N. Hansen, "Water Analog Study of Effects of Gating Designs on Inclusion Separation and Mold Filling Control," AFS Transactions, 1993, 199-209.
254. S.H. Jong and W.S. Hwang, "Measurement of Flow Pattern for the Mold Filling of Castings," AFS Transactions, 1991, 69-75.
255. S. Mishima and J. Szekely, "The Modelling of Fluid Flow and Heat Transfer in Mold Filling," ISIJ Inter., Vol. 29 (4), 1989, 324-332.
256. P.A. Davidson, X. He and A.J. Lowe, "Flow Transitions in Vacuum Arc Remelting," Materials Science and Technology, Vol. 16 (6), 2000, 699-711.

257. L. Zhang and B.G. Thomas, "Fluid flow and inclusion motion during ingot teeming process-Part III: inclusion motion," Report, Continuous Casting Consortium, University of Illinois at Urbana-Champaign, 2005.